Spatial Estimation of Surface Soil Texture and Organic Matter using Hyperspectral Spectroradiometer and Multispectral Landsat-8 OLI Data

By

Saqib Hussain

(2019-NUST-MS-GIS-319187)

A thesis submitted in partial fulfillment of the requirements for the degree of Master of Science in Remote Sensing and GIS

Institute of Geographical Information Systems
School of Civil and Environmental Engineering
National University of Sciences and Technology
Islamabad, Pakistan

May 2023

THESIS ACCEPTANCE CERTIFICATE

Certified that final copy of MS/MPhil thesis written by **Saqib Hussain (Registration No. MSRSGIS 00000319187), of Session 2019 (Institute of Geographical Information systems)** has been vetted by undersigned, found complete in all respects as per NUST Statutes/Regulation, is free of plagiarism, errors, and mistakes and is accepted as partial fulfillment for award of MS/MPhil degree. It is further certified that necessary amendments as pointed out by GEC members of the scholar have also been incorporated in the said thesis.

Signature:

Name of Supervisor: Dr Javed Iqbal

Date: 24 08 2023

Dr. Javed Iqbal
Professor & HOD IGIS, SCEE (NUST)
H-12, Islamabad

Signature (HOD):

Date: 24 08 2023

Dr. Javed Iqbal
Professor & HOD IGIS, SCEE (NUST)
H-12, Islamabad

Signature (Associate Dean):

Date: 24-08-2023

Dr. Ejaz Hussain
Associate Dean IGIS, SCEE (NUST)
H-12, ISLAMABAD

Signature (Principal & Dean SCEE):

Date: 24 AUG 2023

PROF DR MUHAMMAD IRFAN
Principal & Dean
SCEE, NUST

DEDICATION

To

My Sweet and Loving Family

Thanks for their love, care, and motivation since the start of my studies, and

to all those who encouraged me and prayed for me for the completion of this

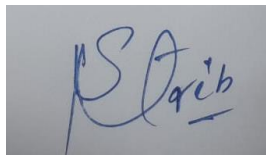*thesis.*

ACADEMIC THESIS: DECLARATION OF AUTHORSHIP

I, Saqib Hussain, declare that this thesis and the work presented in it are my own and have been generated by me as the result of my original research.

Spatial Estimation of Surface Soil Texture and Organic Matter using Hyperspectral Spectroradiometer and Multispectral Landsat-8 OLI Data

I confirm that:

1. This work was done wholly by me in candidature for an MS research degree at the National University of Sciences and Technology, Islamabad.

2. Wherever I have consulted the published work of others, it has been attributed.

3. Wherever I have quoted from the work of others, the source has been always cited.

4. I have acknowledged all main sources of help.

5. Where the work of the thesis is based on work done by myself jointly with others, I have made clear exactly what was done by others and what I have contributed myself.

6. None of this work has been published before submission. This work is not plagiarized under the HEC plagiarism policy.

Signed:

Date: 28/08/2023

ACKNOWLEDGEMENTS

Table of Contents

List of Figures

List of Tables

LIST OF ABBREVIATIONS

Abbreviation	Explanation
WD	Soil Wetness / Doughtiness
Ca	Calcium
ºC	Degree Celsius
TX	Topsoil Texture
cm	Centimeters
km^2	Square Kilometer
log	Logarithm
m^3	Cubic Meter
mg	Milligram
ml	Milliliter
S	Sand
C	Clay
LS	Loamy Sand
SC	Sandy clay
ZC	Silty clay
OL	Organic Loam
SL	Sandy Loam
SZL	Sandy Silt Loam
CL	Clay Loam
ZCL	Silty Clay Loam
ZL	Silt Loam
SCL	Sandy Clay Loam
POR	Soil porosity
POR-P	Poor-< 0.5% bio pores at least 0.5mm in diameter
POR-G	Good-> 0.5% bio pores at least 0.5mm in diameter
F	Fine (more than 66% of the sand < 0.2mm)
C	Coarse (more than 33% of the sand > 0.6mm)
M	Medium (< 66% fine sand and < 33% coarse sand)
VC	Very coarse
CO_2	Carbon Dioxide
GH	Gravel with non-porous (hard) stones
GS	Gravel with porous (soft) stones
GPS	Global Positioning System
HCO_3	Bicarbonate Ion
IDW	Inverse Distance Weighted
MS	Microsoft
N	North
NO_3^-	Nitrate ion
r^2	Coefficient of Correlation
RMSE	Root Mean Square Error
MEE	Mean Estimation Error
MAEE	Mean Absolute Estimation Error

SD	Standard Deviation
UC	Union Council
UTM	Universal Transverse Mercator Projection
ASD	Standard Res Analytical Spectral Devices
γ, γm	Unit weight, bulk unit weight, moist unit weight
γd	Dry unit weight
γsat	Saturated unit weight
W	Total weight of soil
Ws	Weight of solid particles
WW	Weight of water
V	Volume of soil
Vs	Volume of solid particles
Vv	Volume of voids
Vw	Volume of water
S	Degree of saturation
w	Water content or moisture content
G	Specific gravity of the solid particle
ρ	Soil Density
e	Void ratio
w	Water content or moisture content
SOC	Soil Organic Carbon
R-squared (R^2)	Coefficient of Determination
MLR	Multiple Linear Regression
P Value	Level of marginal significance
SA	Spatial Auto Correlation
OLS	Ordinary least squares
GWR	Geographically Weighted Regression
WB	World Bank
ADB	Asian Development Bank
UN	United Nations
GMDH	Group Method of Data Handling

ABSTRACT

Fine-scale soil spatial variability mapping is one of the prerequisites for adopting precision agriculture. This study used a hyperspectral radiometer and satellite remote sensing data for fine-scale surface soil texture and organic matter. A total of 626 surface soil samples (7cm depth) were collected and analyzed for soil texture and organic matter in the Lab. Multiple linear regression (MLR) statistics were used to relate soil spectral data derived from multispectral LandSat-8 OLI imagery data and hyperspectral remote sensing data of ASD FieldSpec Spectroradiometer with sand, silt, clay, and organic matter data. The MLR analysis of Multispectral data of Landsat-8 OLI satellite showed a significant relationship ($p < 0.05$) with band-5, band-7, and band-11 with sand% ($R^2 = 0.558$), clay% ($R^2 = 0.589$) and O.M.% ($R^2 = 0.687$). The MLR analysis of hyperspectral remote sensing data of ASD Field Spec spectroradiometer showed a relationship with a different significant level of wavelength X1362, X1366, X1843, and X1856 with sand% ($R^2 = 0.370$), wavelength X1830, X1839, X1873 and X1882 with clay% ($R^2 = 0.317$) and wavelength X 1363, X1833, X1886 and X1909 with O.M.% ($R^2 = 0.440$). A soil texture map of the entire study area was developed in GIS using the USDA-ARS soil texture triangle. The findings imply that remote sensing and geographical information system approaches might be employed to map the soil surface texture and O.M. over a wider area at a fine scale.

INTRODUCTION

1.1 Importance of Study

One significant soil characteristic that affects stormwater infiltration rates is soil texture. Sand, silt, and clay content together make up a soil's textural class. The four main textural classes of soils are (1) sands class, (2) silts class, (3) loams class, and (4) clays class. The significance of the texture of the soil, various methods for determining the texture of the soil, and the significance of soil texture in managerial choices.

Several soil properties are impacted by texture, including Drainage, water holding- Capacity on the surface, Aerating, Erosion of soil, Organic matter, and pH in the soil. The speed at which water permeates soggy soil depends on the texture of the soil; Sandier soils allow water to flow more freely than clayey ones do. The amount of water that is available to the plant when the field's capacity is reached depends on the soil's texture; clay can hold more moisture than sandy soils. Furthermore, soils with good soil aeration—a condition in which the drained soil air is related to that in the atmosphere are frequently well-drained. This air is beneficial for plants' root development and, consequently, crop health. A soil's erodibility (susceptibility to erosion) varies according to its soil texture; In the same conditions, silt and clay-rich soils are more erodible than sandy soils. Organic matter breaks down more rapidly in sandy soils than in good soils under similar environmental conditions, tillage practices, as well as fertility management due to the greater oxygen available for the procedure in the sandy soils. The percentage of clay and organic matter affects the soil's ability to exchange cations, and these two factors also affect a soil's ability to buffer pH changes brought on by incorporating lime. SOM in the soil is an important part of the soil. It contains nutrition for crops as it

decomposes and contributes to the cation complex necessary to hold imposed nutrients in the soil. Improved soil aggregation from higher organic matter content maintains the structure of the soil, drains, and oxygenation, all of which are necessary for high crop yields. Increased moisture retention and, as a result, the crop's ability to withstand drought are two additional effects of soil organic matter. An adequate amount of organic matter in the soil will make it easier to work with and plough, less erodible, and better at retaining nutrients. Other benefits include improved crop yields, higher fertility, better crop root growth, and resistance to soil crusting and compaction. Organic residues must be added to the soil to improve and maintain it. Excessive tillage, contemporary monoculture, and reduction rotation cropping are examples of fact matter amounts to fall below optimal levels. Row cropping also leaves behind less organic matter in the soil than is traditionally needed to keep acceptable levels. Grass forages and legumes, in contrast to row crops, have thick, fibrous root systems that produce a significant amount of organic residue. Forage or legume-based crop rotations will help to maintain SOM, enhance the soil content, and consequentially should increase the yields of crop. A good source of organic residue is manure, which enhances soil quality. A large amount of research has been done using Remote Sensing Images to predict soil properties, Interpolation techniques are common way to map soil properties for large area from a limited data set, with advancement in Geo-Spatial sensors and machines, new methods have evolved, among which spectro-radiometry is common technique. Below we will see some examples by which soil studies have been done using GIS & Remote Sensing. In research published in Geoderma Journal titled "Using hyperspectral images and field measurements in multivariate regression modelling, high resolution topsoil mapping" found the effective utilization of hyperspectral remote sensing image to estimate Organic matter of the soil and texture of the soil. It also explored estimation of sand content, clay content, organic carbon content, and the nitrogen (N) predicted using PLSR and MLR.

1.2 Background Information

All over the world, sustainable agriculture sector is the most important objective. Even though agricultural productivity has increased significantly over the past 50 years, rapid population expansion, natural disasters, and climate change continue to pose a threat to global food security. (Ren et al., 2019) An important part of getting healthy soil and a good crop yield is treating the soil properly for healthy growth. Considering the rising demands for both temporal and spatial resolution regarding soil surface characteristics in the multiple different applications for precision agriculture, conventional research lab techniques to be proving to be insufficient. This has been the key focus for soil researchers and environmental stakeholders during recent decades. (Ehsani et al., 1999) Furthermore, compared to more conventional techniques, the expenses of soil analysis using precision agriculture technologies are relatively high. (Ge et al., 2011) Crop yield is strongly affected by the elimination of nutrients from soil, which has an impact on a nation's economy. Nowadays, it is common practice to monitor crops' health and productivity using remote sensing technology. (Rembold et al., 2015) To efficiently investigate soil texture and organic matter (O.M.) properties and to suggest a solution to improve crop production by enhancing the effectiveness of soil physical properties in an efficient way, a different approaches and techniques have been developed. In this regard, various techniques for exploring soil properties can be investigated within the field of remote sensing. (Galvaoet al., 1997) A field's soil characteristics may demonstrate fine-scale spatial patterns that can be determined through remote sensing. (Mulla et al., 2000) The technology has accelerated traditional soil surveying by significantly decreasing the amount of field work. (Manchanda et al., 2002) Unless the soils are completely covered by massive shrubs and thick canopy trees, optical technologies including aerial imagery, multispectral imagers, and hyperspectral sensor systems can be employed to capture the reflectance signatures for investigating topsoil attributes. (Jensen, 2000) Several soil-related parameters, comprising

surface soil condition, soil texture, organic matter, colour, mineralogy, iron and iron oxide content, soil moisture, influence the spectral response of soil. (Dwivedi, 2001) Beginning in the early 1980s, spectral signature reflectance data used to analyse the soil characteristics. (Krishnan et al., 1981) and (Pitts et al., 1986) studied soil organic matter using near infrared reflectance (NIR). (Ben-Dor and Banin. 1995) Several soil parameters, including specific surface area, clay content, hygroscopic moisture, cation-exchange capacity (CEC), calcium carbonate concentration, and O.M. were determined using NIR spectroscopy of soils. (Viscarra-Rossel and Mcbratney 1998) Clay content, soil moisture, and O.M. were analysed in Soil Samples taken Australia. To analyse these parameters, they employed the spectral signature determined from 1300 nm to 2500 nm at 2nm intervals. They found that clay and moisture concentrations could be predicted most accurately at 2100 nm, While the low accuracy both parameters was found at 1600 nm. These wavelengths did not reveal any conclusive association with O.M. The study of soil properties has consistently made use of satellite remote sensing data. (Hong et al. 2002) By examining the associations between signatures of spectral reflectance and variables of soil using geo-statistical analyses, such as Multiple Regression, Simple Correlation, and Principal Component analysis (PCA), investigated capability of hyperspectral data to calculate the soil's EC and fertility levels. The satellite RS data were compared to field estimated soil properties. For Mg and CEC, the correlations to the hyperspectral band were found to be the strongest. PCA revealed that PC 2 and PC 4 were highly effective in elucidating soil variation for cation-exchange capacity, magnesium, Organic Matter, potassium, and pH. (Shepherd and Walsh 2002) used a Spectroradiometer library to determine the qualities of soil. They used diffusion reflectance spectroscopy analysis as the foundation for their work. (Nanni and Dematte 2006) studied the characteristics of topsoil of Brazilian using the soil satellite reflectance measurements from Landsat TM imagery. Chemical analysis of samples of soil taken from the surface (0–20 cm)

even below (80–100 cm) soils was followed by Statistical analysis using the reflectance values of the soil to generate Multiple Regression Analysis. Most soil characteristics, including clay, iron oxides (Fe203), and titanium dioxide, may be predicted by these regression equations (Ti02). (Hashemi et al. 2007) 63 samples of soil (10 cm depth) were taken using Global position System, and satellite images from the year 2002 were used to develop a soil mapping model for the Sarvestan plain in Iran using Landsat TM satellite images and field measurements. Band 6 and gypsiferous soil were shown to be strongly correlated in the study, as well as the spectral ratios (band 3-band 4-band 2-band 4) and soil EC in the area. Utilizing ILWIS software's statistical methods, supervised classification was accomplished. Gypsum and EC maps both have overall accuracy of 80.56% and 78.57%, respectively. One essential factor of soil's physical property is its texture. It affects numerous additional soil characteristics that are essential for crop yield and research area treatment. (Brown, 2003) Physical properties of soil distribution have a significant impact based on its reflection characteristics. (Hoffer. 1978) assumed that the key variable influencing soil reflectance was its silt concentration. He observed that as the silt percent decreases, the soil reflectance also decreases. (Baumgardner et al. 1986) For all wavelengths between 0.4 and 1.0 μm, it was shown that a substantial exponential growth is detected due to a reduction in particle size. (Palacios-Orueta and Ustin 1998) By investigating correlation between soil characteristics and radiometer reflectance signature data obtained with the AVIRIS (Advanced Visible/Infrared Imaging Spectrometer), it was discovered soil surface texture, organic matter, and iron levels was the key elements determining the spectral signature curve of soil. (Okin and Painter 2004) used the same data to determine visible surface reflection to analyse the useful sand grain size in sand plumes at a location in the Mojve Desert. They observed an influential negative association between sand particle size in plumes and reflectance signature values. As per correlation study, the most important wavelength for predicting is short wave infrared. A key determinant of soil fertility

and health is soil O.M. The availability of organic matter in the Soil has influential effect on the colour of the soil's properties. In general, the amount of organic matter in the soil appears to increase as the darker colour of a soil. A research project by (Coleman and Montgomery 1987) indicated that a decrease in reflectance values is generally caused by an increase in moisture in the soil and O.M. They observed that band 1 (450–520 nm) as well as band 4 are the best wavelength bands for predicting O.M. (760- 900 nm), utilising a multi - band radiometer with a band configuration corresponding to the Landsat Satellite sensor.

(Mirzaee et al., 2016) In agronomical and environmental studies, it's crucial to estimate organic matter in soils (SOM) in areas that haven't been sampled. Geostatistical techniques like Ordinary Kriging (OK), Simple Kriging (SK), and Cokriging (CK), as well as composite techniques like Regression-Simple Kriging (RSK)/-Ordinary Kriging (ROK), and Artificial Neural Network-Simple Kriging (ANNSK)/-Ordinary Kriging (ANNOK), were examined for their ability to investigate soil organic matter characteristics. The derived models was evaluated using three performance criteria: coefficient of determination, root mean square error, and mean error R^2.It was determined that data from Landsat ETM+ images could be used as ancillary variables for improving spatial prediction and monitoring soil Organic matter, and generating accurate soil organic matter maps, this is the first stage in the site-specific management of soil. (Liao et al., 2013) The purpose of this study used a small sample of soil that was collected from a site in the Chinese city of Pingdu to analyze Landsat (ETM) remote sensing imagery as ancillary parameters for spatial estimate of surface soil texture. The given approaches to measuring surface soil texture variation were examined: (1) Based on the correlation among soil surface sand, silt, and clay compositions and remote sensing data, multiple multiple regression analysis (MSR) was performed. (2) Sand, silt, and clay composition of surface soil are correlated with remote sensing data. When kriging and multiple stepwise regression (MSR) are used with remote sensing data, estimations of surface soil

texture are significantly improved. (Bousbih et al., 2019) For the estimation and mapping of soil content (texture), using data of radar and remotely sensed optical data from Sentinel-1 (S-1) and Sentinel-2 (S-2). (Ahmed & Iqbal, 2014) In this study the potential for Remote Sensing and (GIS) methods in examining the variation of surface soil in space properties is explored. Surface soil characteristics and spectral data from the Landsat TM5 satellite were related using a multivariate linear regression (MLR) analysis technique. The results show that RS and GIS approaches can be employed to map the soil texture and Organic matter over a larger area at a fine scale. (Shahriari et al., 2019) This study's goal was to evaluate how the percentages of sand, silt, and clay will be spatial distributed over the Sistan floodplain. The soil texture components were mapped using the Random Forest (RF), Regression Kriging-Neural Network Residual Kriging (RKNNRK), Neural Network Residual Kriging (NNRK), Regression Kriging (RK), and Cokriging (COK) methods. The results demonstrated that Neural Network Residual Kriging (NNRK) and Regression Kriging-Neural Network Residual Kriging (RKNNRK) models produce more accurate results combined with data from remote sensing and can therefore use for suitable mapping of soil particles at the regional and floodplain scales. (Song et al., 2017) To forecast the geospatial variation of soil organic matter (472 samples at 0-20 cm) in Shaanxi, China, an Extreme Learning Machine-Ordinary Kriging (ELMOK) hybrid geo-statistical technique was presented. Remote Sensing data and environmental factors used to generate a total of 14 auxiliary variables (predictors). Conventional geo-statistical techniques, such as Simple-Kriging (SK) and Ordinary-Kriging (OK), as well as hybrid-geostatistical approaches like Regression-Ordinary Kriging (ROK) and Artificial Neural Network-Ordinary Kriging, were compared to the suggested method (ANNOK). The results showed that principal components (PCs) were used as input parameters in the extreme learning machines (ELM) model. They performed better in both Artificial-Neural-Network (ANN) and Multiple-Linear-Regression (MLR) models. The ELMOK model showed the minimum Root-Means-Square-

Error (RMSE = 1.402 g kg1) and the Maximum co-efficient of determination (R^2 = 0.671) when compared to geo-statistical and hybrid-geostatistical prediction techniques of soil organic matter spatial distribution. In conclusion, factors derived from remotely sensed data have improved our comprehension of the spatial variability of SOM contents. (Vibhute, Dhumal, et al., 2018) SOM assessment is a time-consuming process because of its extensive spatial variability and chemical processing. Without using nasty chemicals, Visible-Near Infrared (VNIR) Reflectance Spectroscopy (RS) has traditionally been used to measure the soil's organic content. The Analytical-Spectral-Device (ASD) Field Spec 4 spectroradiometer was used in the current study to collect the reflectance spectra of thirty soil samples taken from the study area in the Aurangabad region of Maharashtra, India's Phulambri Tehsil. This method was used to locate the 400-2450 nm wavebands' absorption channels. The Savitzky-Golay (SG) technique with First-derivative transformation was used to smooth the spectra (FDT). By performing an analysis among spectral signatures reflectance and soil organic matter contents, the Partial Least Squares Regression (PLSR) model used to anticipate the mean-Square Error (RMSE) for the pretreatment co-efficient of determination both was before and after determinate 0.66 and 0.77 respectively. SOM was shown to have sensitive channels wavelengths of 441nm, 517nm, 527nm, 648, and 1000nm. Study will help with decision-making and efficient, economical farming. (Alexakis et al., 2019) Along with salinization, compaction, a loss in soil organic material and soil erosion is a major risk in the Mediterranean region and one of the main causes of degradation. Several soil characteristics, including calcium carbonate equivalent (CaCO3), Organic Matter of soil, texture of soil, and permeability, can be used to evaluate soil erosion. In this study, the potential for numerous cutting-edge techniques Satellite Imagery, Field spectroscopy, Soil Lab analysis, and GIS) to monitor soil organic matter, calcium carbonate, and soil erosion (K-factor) of the Akrotiri cape in Crete, Greece, was examined. Mapping of soil organic matter, calcium carbonate, and soil

erosion was made possible via lab analysis and soil spectral reflectance signature in the VIS-NIR using Landsat-8, Sentinel-2, or field spectroscopic data, Machine Learning, and geo-statistics. Finally, to evaluate the potential contribution of various ways in calculating soil erosion rates, Ordinary-Least-Square-Regression (OLSR) and Geographical-Weighted-Regression (GWR) procedures used. The resulting maps accurately depicted the spatial distribution of the Soil organic matter, calcium carbonate, and soil erosion in the GIS environment. Findings can help in the design of effective erosion control strategies and sensible planning for land use in the study area. (Bousbih et al., 2019) The prediction and soil texture mapping with remotely sensed optical and radar data is explored in this work. The analysis relies on Sentinel-1 and sentinel-2 data collected across a semi-arid region of around 3000 km2 in central Tunisia from July to the beginning of December 2017. Techniques based on the random forest (RF) and vector support machine (SVM) methods are proposed for the classifying and visualizing (Mapping) of clay content. Both methods are evaluated using a three-fold cross-validation. The indicator for soil moisture obtained sentinel 1 and sentinel 2 data results in the classification with the best performance, with overall accuracy (OA) values of support vector machine and random forest classifications of 63% and 65%, respectively. (Nanni & Demattê, 2006) Traditional soil analyses can produce environmental pollutants and are costly and time-consuming. This study's goal was to create and assess an approach for measuring soil properties by using reflectance spectral signature as a substitute to conventional techniques. To predict soil attributes using radiometric data, geo-statistical analysis and multiple linear regression equations were developed. Band-22 and 13 RIDs from various optical spectrum ranges of wavelengths were employed in laboratory data. Although, the satellite imagery data is only used for the reflectance of the Landsat-TM bands. Surface and subsurface Soil layers were used to generate multiple regression equations. Laboratory spectral analysis made it possible to estimate some tropical soil physical properties. (Ge et al., 2011)

An effective and precise method for identifying soil properties on the farm is essential to the success of precision agriculture (PA). Applications ranged from bench-top spectrometer-based laboratory examination of soil samples to hyper-spectral satellite imagery-based field-scale soil mapping. The three most popular techniques used for data analysis are MLR, PCR, and PLSR. This article also discussed the limitations and opportunities of employing RS to evaluate agricultural soil properties. (Levy et al., 2014) In the McMurdo Dry Valleys of Antarctica, soil moisture is a spatially heterogeneous quantity that has a significant impact on the local biological population and the permafrost's thermal condition. This study's objective was to look into whether soil moisture status in the Dry Valleys might be determined using hyperspectral remote sensing methods. We evaluated the spectrum reflectance parameters of wet soil samples from the Dry Valleys under the influence of natural light, and we connected diagnostic spectral features to the moisture content of the soil's topmost layer. These findings imply that soil moisture maps of the Dry Valleys could be generated using non-invasive remote sensing methods using airborne hyperspectral imaging of this environment. (Yu et al., 2018) For the management of forestry, agriculture, and the environment, it is essential to map soil attributes quickly and precisely. In this research, a novel hyperspectral remote sensing techniq of predicting soil properties in northwest of the Qinghai-Tibet Plateau, in Shenzha County of the Qiangtang Plateau, was developed and evaluated in Stipa purpurea-dominated alpine grasslands. Analysis was done on the relationships between the soil characteristics and the bands and improved spectral parameters obtained from both field and satellite hyperspectral data. To map the soil properties, regression models that investigate the Correlations were expanded upon. Findings demonstrated that accurate spatial variation of the soil parameters was generated by stepwise regression models based on enhanced spectral parameters derived from hyperspectral Satellite images. According to this study, the hyperspectral data-based approach has a significant deal of potential for predicting the characteristics of the soil.

(Vibhute, Kale, et al., 2018) In soil science, it is difficult and challenging to identify soil physicochemical attributes (SPAs) with accuracy and reliability. The complexity of nature allows for spatial and temporal variations in the SPA. In the past, SPA detection was accomplished using standard soil physical and chemical laboratory analysis. These laboratory techniques, however, suffer from a lack of rapid requirement. Diffuse reflectance spectroscopy (DRS) is therefore a preferable method for nondestructively detecting and evaluating soil physical properties. The VNIR spectrum's quantitative analysis was carried out. The Field Spec 4 spectroradiometer from Analytical Spectral Device (ASD) was used to record the spectra of aggregated agricultural soils. To obtain pure spectra that served as the input for regression modelling, the soil spectral signatures in the VNIR area were preprocessed. The calibration models were built using the Partial-Least-Squares-Regression (PLSR) method and each one was individually verified for the estimation of SPA from the soil spectrum. A study of the correlation between reflected spectral signature and determined SPAs served as the premise for the computed model. The following SPAs were found sand content, silt content, clay content, phosphorus nutrients, potassium nutrients, iron nutrients, electrical conductivity (EC), pH values, Soil Organic Carbon, nitrogen nutrients, Soil Organic Matter. The experimental findings showed that the VNIR-DRS was more effective at detecting SPA and at making predictions for SPA. The methods examined here, in summary, provided quick and novel SPA detection from reflectance spectroscopy. Finding will be useful for decision-making and precision farming. (Vibhute, Dhumal, et al., 2018) Along with good farming practices and soil quality, soil organic matter is important for the development of plants. Using the Analytical-Spectral-Device (ASD) Field spec 4 spectroradiometer, For the purpose of this investigation, the spectral signature of thirty soil samples collected in the Phulambri Tehsil of Maharashtra, India's Aurangabad region, were calculated. By performing a analysis between spectral signature reflectance and soil organic matter content, the Partial-Least-Squares-Regression

(PLSR) model was used to forecast the SOM. The study will help with decision-making and efficient, economical farming. (Virgawati et al., 2018) One of the soil characteristics that affects the majority of soil science processes is texture of soil. To supporting agronomic decisions for farm management, information on soil texture is essential. The goal of the study is to create a soil texture map using inverse distance weighted (IDW) interpolation and lab Vis-NIR (Visible - Near Infra-Red) spectroscopy. We measured the soil reflectance using an ASD Fieldspec 3 with a 350 to 2500 nm spectral range. To measure the silt content, clay content, and sand content, a pipette method was employed. To create a prediction model for soil texture, partial least square regression (PLSR) was used. The predicted values were visualized on a map, revealing details about the temporal and spatial variability of soil texture.

1.3 Objectives of Study

The objectives of the study were to:

a. Relate surface soil texture and organic matter with hyperspectral ASD Filedspec and Landsat-8 OLI data.

b. Map surface soil texture and organic matter of the study area.

MATERIALS AND METHODS

2.1 Study Area

The area of the study, which occupies an area of about 1060 km2, is a subunit of Shakar Garh district in Narowal, Punjab, Pakistan in (Figure 2.1) describes in detail. Ravi River in the south and the Jammu-Kashmir border in the north increase's importance from strategic viewpoint. From this, Pakistani Standard Time is calculated (Haider et al., 2016). Major crops grown in these abundant include wheat, rice, guava, citrus, and mango and fertile lands with loam clay soil and plain topography. Water tables range in depth from 40 to 50 feet, and tube wells are the primary source of irrigation (Tariq, et al., 2013). According to (Ali, et al.2020) the peak temperature in the summer is (42 $^{\circ}$C) and the lowest recorded annual rainfall is (4 $^{\circ}$C) (Punjab Development statistics). Shakargarh became tehsil in 1853. It's literacy rate is percent. Sialkot tehsil of sialkot district was transferred to Gurdaspur District and it remained an administrative subdivision of Gurdaspur district until partaion in 1947.Under the Radcliffe Award, there of the four tehsil of Gurdaspur distrcit on the easten bank of the Ujh river – Gardaspur, Batala and Pathankot – were awarded to India and only one, Shakargarh, was assigned to Pakistan. After the creation of Pakistan, Shakargarh became a part of Sialkot district one again. In July 1991, two teshsils (Narowal and Shakargarh) were spilt off from Sialkot district and Shakargarh became a tehsil of the newly formed Narowal district. Later, in July 2009, Tehsil Zafrwal was created. At present, Narowal is functioning as a separate administrative district with effect from July 01, 1991.
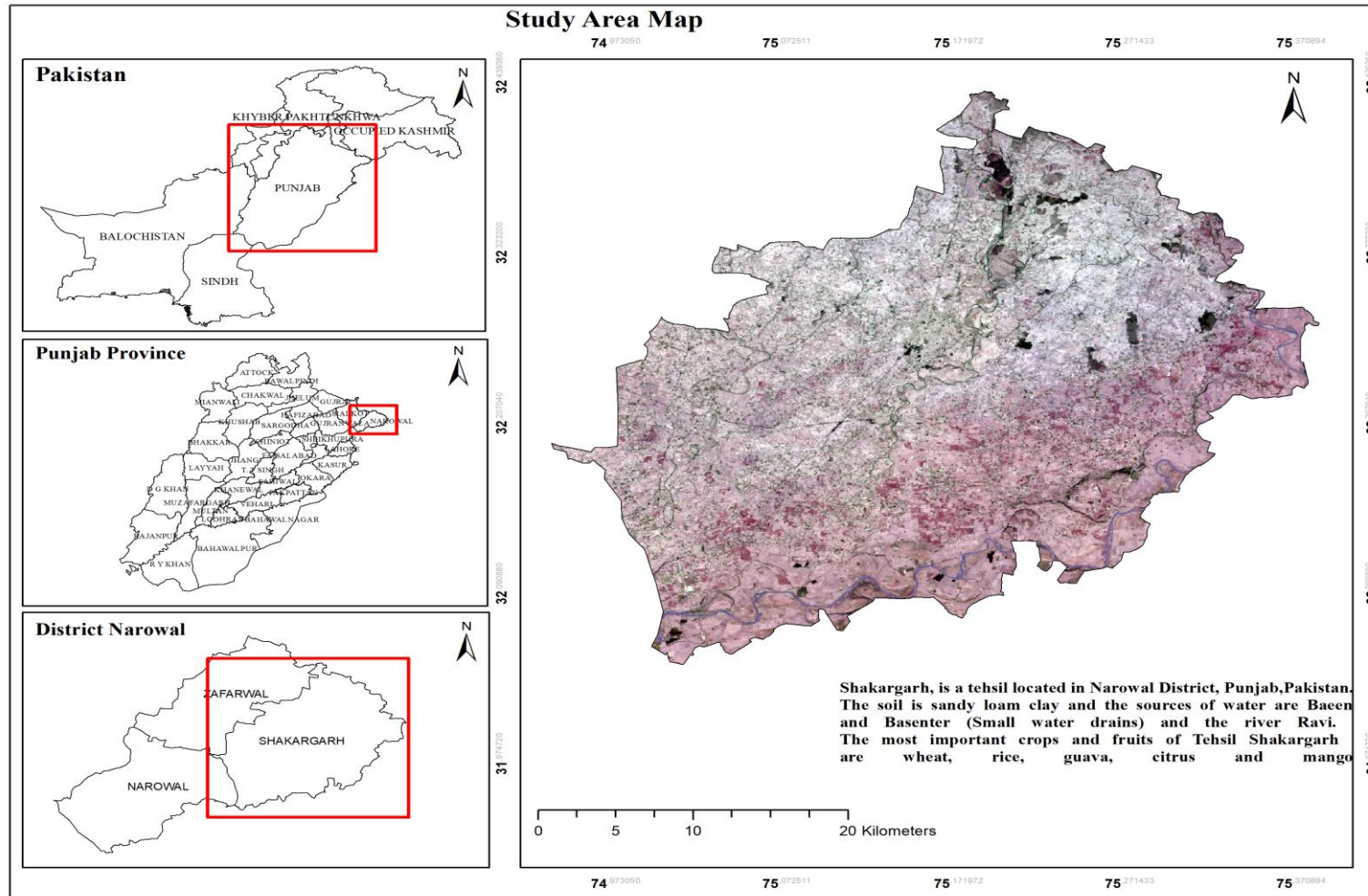
Figure 2.1. Location map of the study area (Tehsil Shakargarh, District Narowal, Punjab).

2.2   Methodology and Data Set

Soil samples are collected from predefined areas in a field on the bases of Soil variation and sent to Lab for analysis of soil parameters (Soil Texture and Organic Matter). After that detected the Radiometry reflectance values (Soil Texture & O.M.) of these samples through Spectroradiometer. The Multispectral LandSat-8 OLI image downloaded from USGS earth explorer and after downloaded then image pre-processing done by using Erdas Imagine software, this image used to remotely sense surface attribute of soils. Multiple linear Regression Analysis Spatial Modelling is used to generate soil texture and Organic Matter Maps. Figure 2.2 depicts a general overview of methodology used in later sections in detail and Figure 2.3 explains in detail a list of software's, and data sets used in the research. The data set and software which are used for this study mentioned figure 2.3. Firstly, soil chemical properties data are required which are collected from filed and then analyzed in the soil lab for Organic matter and soil texture. Secondly Remote sensing data (Imagery and Non-Imagery) are required. Imagery data Multispectral satellite Imagery Landsat-8 having 30-m spatial resolution, 11 bands (430 nm to 1251 nm) acquire from USGS earth explorer, Non-Imagery Hyperspectral remote sensing data acquire using ASD FieldSpec4 having spectral range 356 nm to 2500 nm with 1 nm band width.

ArcGIS pro (Esri, 2023) software is used for geospatial analysis, and Erdas Imagine is used for satellite imagery analysis. SAS (Statistical Analysis System) statistical software used for statistical analysis.
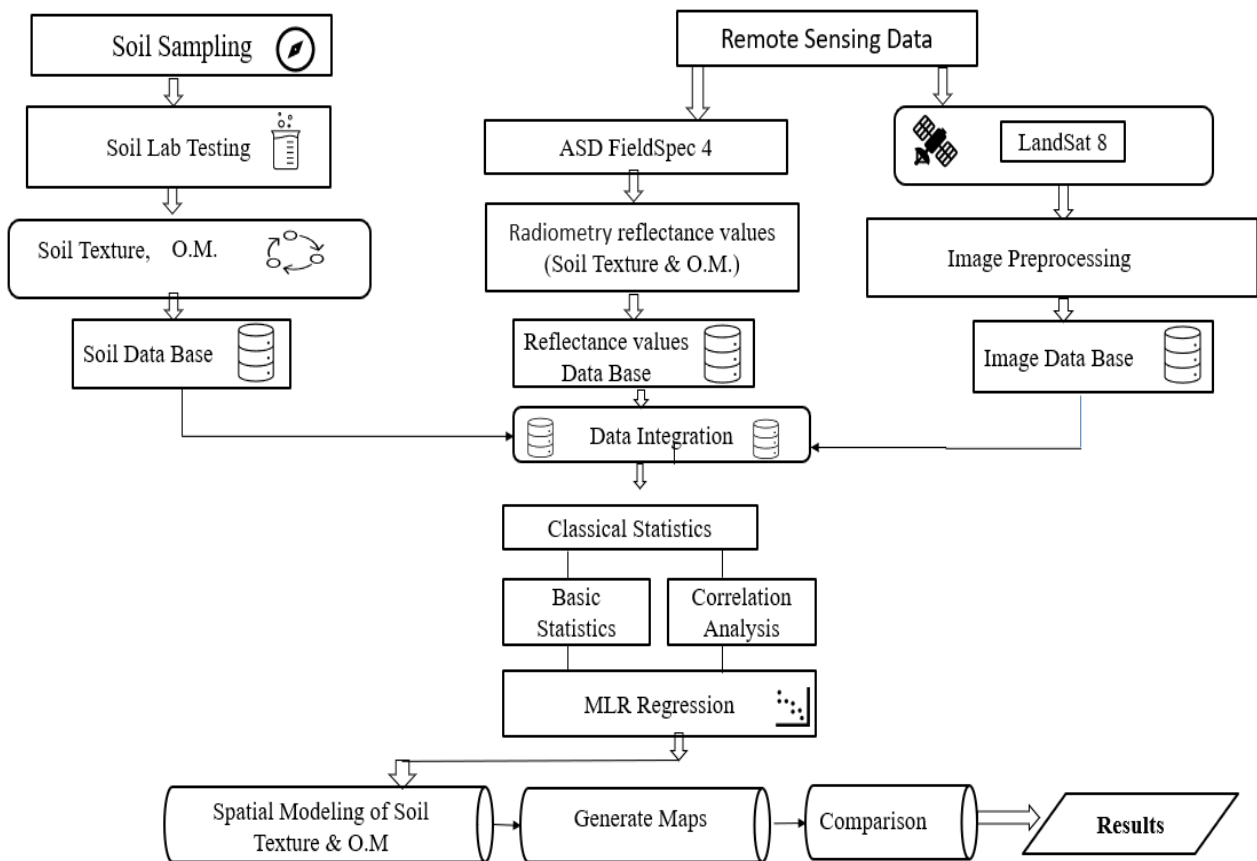
Figure 2.2. Methodological workflow of the study.

Table 1. Detailed list of software, and data sets used in the research.

Data	Description	Source
Soil Chemical Properties	Soil samples collected from the field, analyzed in the lab for soil O.M and soil texture	Field survey
Multispectral Satellite Imagery - Landsat 8	30-m spatial resolution, with 11 bands (430nm to 1251nm)	United States Geological Survey https://earthexplorer.usgs.gov/
Hyperspectral non-imaging remote sensing data	Spectral rang 356 nm to 2500 nm with 1 nm band width	ASD-Field Spec4(Handheld Spectroradiometer)
Software Used		
ArcGIS Pro	Geospatial analysis	ESRI
Erdas Imagine	Satellite imagery analysis	Intergraph and ESA

2.3   Data Processing and Analysis

2.3.1   Surface Soil Sampling

Soil samples have been collected from the field. Every reference field is, 3 to 5 surface ground samples were taken inside a 20 feet diameter of circle from the surface soil (7 cm depth) based on an examination of soil profile textural changes visually and then make 1 composite sample. For decrease the possibility of bias and make sure the sample is distributed evenly, we have used stratified randomly sampling techniques for each reference field. Standard precautionary measures adopted while performing sampling. Figure 2.3 depicts a sampling Activity show.

Instruments from the Geo-Tech Lab, NUST Institute of Civil Engineering, and Narowal Soil fertility Department were used to collect soil samples. Below are the instrument details.

- Core Cutter
- Ramer
- Balance
- Digging tool
- Soil Auger

Different Obstacles were encountered during the survey because local protests blocked the roads. A soil survey sheet was created and is attached as Annexure A. The heat during this task was a significant challenge.

2.3.2   Soil Laboratory Analysis

To determine soil texture, soil samples were brought to the lab in airtight bags and treated to the oven dry method (Zhang, 2011), sieve crushing (Beuselinck, et al., 1998), and hydrometer analysis (Wen, et al., 2002). The Walkley-Black chromic acid wet oxidation method (Schumacher & B.A, 2002) was used to calculate soil organic matter (OM). The relative proportion of sand, silt and clay in soils determines soil texture and affects soil

characteristics such as nutrients retention and leaching and water holding capacity and drainage. The hydrometer method of particle size analysis determines the following classes: sand content (2000 - 50 m), silt content (50 - 2.0 m), and clay content 2.0 m based on the size distribution of these soil particles physically as determined by their rates of taking place in an aqueous solution. This method makes use of an ASTM 152H-Type hydrometer and assumes a standard temp of 20 Celsius and a density of 2.65 g cm-3the measurements are given in terms of grammes of soil for every liter. Hydrometer diagram, Figure 2.4

Calculations

Report results to the nearest 0.1% content:

1. Sand % = ((oven dry soil mass) – (Rsand – RC1)) / (oven dry soil mass) x 100

2. Clay % = (Rclay – RC2) / (oven dry soil mass) x 100

3. Silt % = 100 – (Sand % + Clay %)   (Gavlak, R. et al., 2005)

When sulfuric acid is present, OM is oxidized with a known quantity of chromatic., the amount of oxidizable organic matter that results is measured using the Walkley-Black method. At a wavelength of 600 nm, the remaining chromate is identified spectrophotometrically. The organic carbon calculation is based on organic matter having a carbon content of 58%. The method has a detection limit of approximately 0.10% and, on homogenous sample material, is generally limit of approximately within 8%. Samples with concentration greater than 15% O.M. are best tested by the Loss-on-Ignition (OM_LOI) method (1934; Walkley, A.J.; Black, I.A.). Figure 2.5 shows the soil fertility laboratory's analysis of the organic matter and soil texture.

(a)

(b)

(c)

Figure 2.3. (a), (b) and (c) Sampling activities.

(a)

(b)

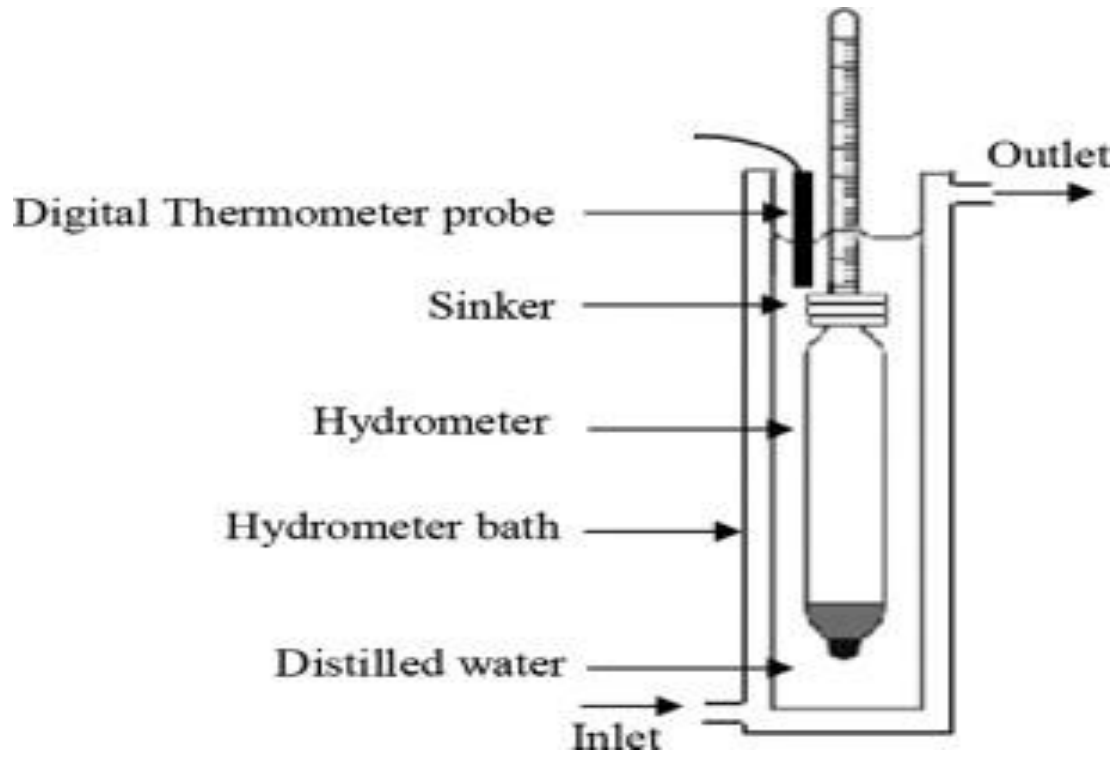Figure 2.4. (a) and (b) Soil texture and organic matter analysis in lab.

Figure 2.5. Hydrometer diagram.

Source: https://d3jlfsfsyc6yvi.cloudfront.net/image/mw:1024/q:85/https%3A%2F%2Fhaygot.s3.amazonaws.com%3A443%2Fcheatsheet%2F10670.jpg

2.3.3   Remote Sensing Imagery Data

Remote sensing of soil surface attributes was conducted using multispectral Landsat-8 OLI data. Multiple factors went into the selection of the spectral data. First, the images were checked for atmospheric disturbance. The entire study area was made sure to be clear of any clouds, haze, or fog. Second, In the study area's maximum pixels of bare soil was intended to be extracted. The existence of vegetation features, water features, and other land contents affects the spectral behavior of soil. Satellite Landsat images were collected for the month of May 2021 to have the least amount of vegetation. The maximum amount of fallow land is available during this period between Rabbi and Kharif.

2.3.3.1 Data pre-processing

The image was taken during the maximum of the fallow season, the Erdas Imagine software's nearest neighbor algorithm was used to suppress pixels of sparse vegetation by primarily using pixels of bare soil. The image was processed through a 3x3 haze reduction filter as part of a spatial enhancement process. The radiometric calibration of bands-1 to band-11 was executed using the suggested techniques by (Czapla-Myers et al., 2015). The proposed operational algorithm was used to produce reflectance images of bands 2 to 7, 10, and 11 after atmospheric correction. The Digital number values in the necessary bands also were calibrated from 0 to 100 to be used with the reflective values of the other bands.

2.3.3.2 Extraction of vegetation and Water

The Normalized Difference Vegetation Index (NDVI) was used to extract the vegetation pixels that were left after the Neighborhood Algorithm application. Normalized Difference Vegetation Index is an indicator that uses the electromagnetic spectrum's red and near-infrared reflection to find vegetation. It is based on the monitoring that in plants that are

actively growing, chlorophyll in the leaf absorbs light in the visible (RED) region of the spectrum while the leaf's mesophyll structure highly reflects light in the near infrared (NIR) region. The most important sign of healthy vegetation is this variation in reflection. Eq. (1) (Karaburun, 2010) provides the NDVI calculation formula.

$$NDVI = (NIR\text{-}Red) / (NIR\text{+}Red) \ldots\ldots\ldots \quad Eq. (1).$$

where:

NIR = reflection in NIR region.

R = reflection in RED region.

The NDVI value can theoretically range from -1 to +1. However, NDVI values of -1 to 0 indicate the presence of water, snow and cloud, Values 0 to 0.2 indicate the presence of Barren Land, built up and rock and values 0.2 to 1 indicate the presence of vegetation. Figure 2.6 shown the vegetation and water.

2.3.3.3 Preparing the non-analysis mask

The existence of water, vegetation water, and other land features has a significant impact on the reflectance characteristics of soil. Results from such land features' reflection data may have mixed spectra. By creating a non-analysis mask in ArcGIS, such different features in land were thus excluded from the analysis. Using NDVI, natural vegetation and water bodies were extracted. Land use maps generated by the National survey organization; the study area's exact built-up area boundaries were digitally recorded. (i.e., Survey of Pakistan). Thus, by combining these datasets, a non-analysis mask was generated that included water, natural vegetation, built up areas and forests. Figure 2.7 depicts a bare soil map.
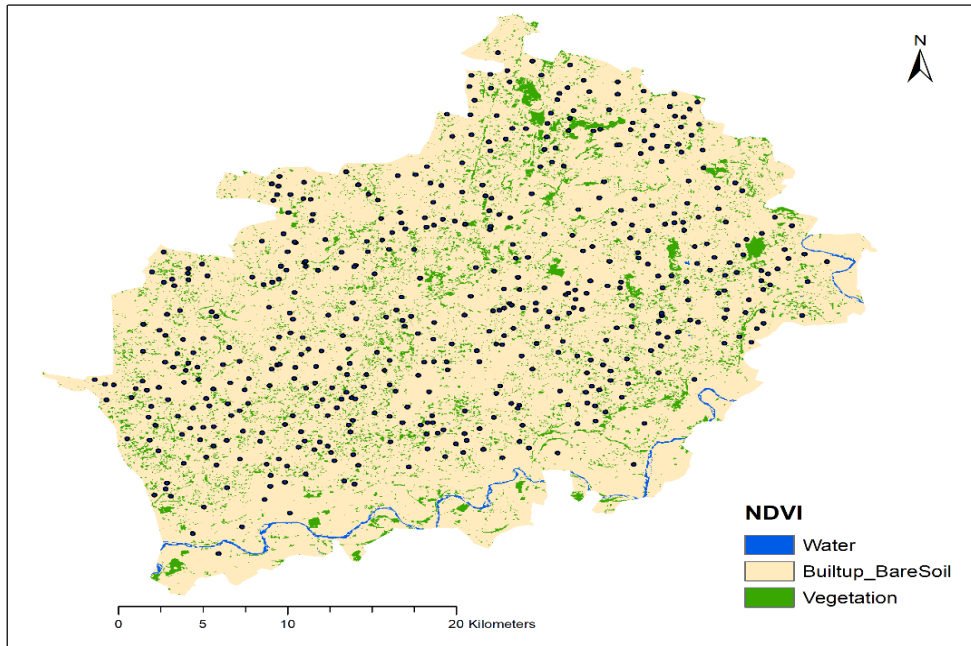
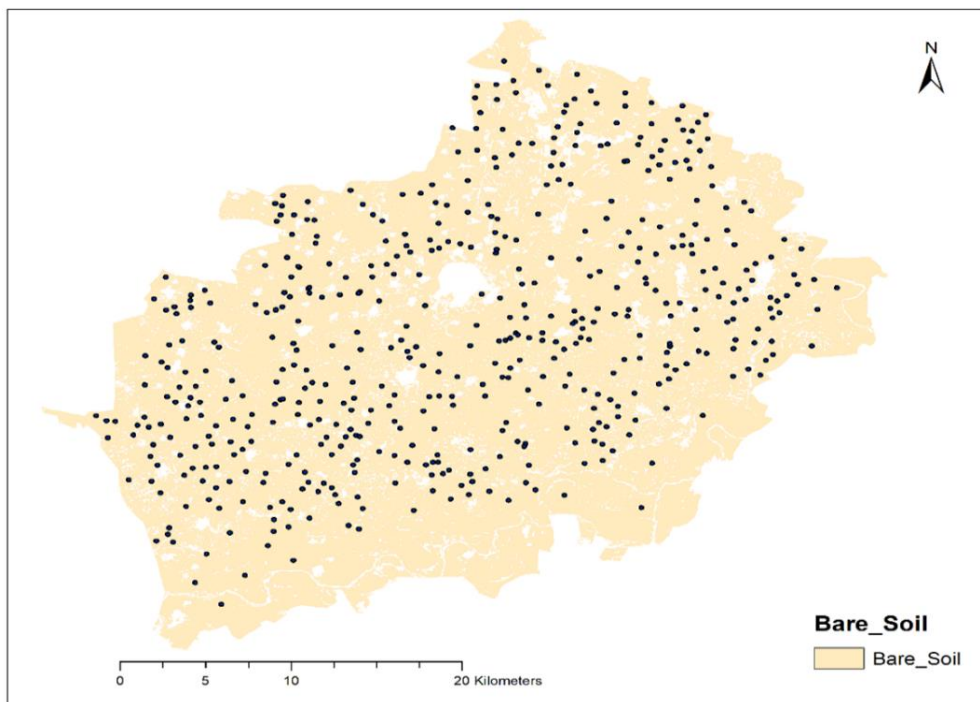Figure 2.6. Extraction of vegetation and water.

Figure 2.7. Bare soil map.

2.3.4 Remote Sensing Non-Imagery Data

The ASD Fieldspec 4 hyperspectral spectroradiometer provides performance across the 3nm VNIR, 8 nm SWIR spectral resolution and the full-spectrum solar irradiance (350 - 2500 nm). For the detection and identification of substances having specific spectral characteristics at longer wavelengths, such as alteration minerals, atmospheric analysis, and gases, the improved spectral resolution in the SWIR range (1000 - 2500 nm) is particularly helpful. The ASD Fieldspec 4 hyperspectral spectroradiometer is a solid solution for ground truthing, spectral library building, sensor validation, and calibration because it has an 8 nm resolution that is equal to or greater than the spectral resolution of the most of hyper-spectral sensors. The ASD Fieldspec 4 hyperspectral spectroradiometer can be employed as a high-resolution spectro-meter for extremely precise measurements of contact reflectance, just like all other ASD Field Spec Spectroradiometers.

2.3.4.1 Soil Sample Preparation

Soil samples are left to dry, ground, and sieved before analysis. A homogeneous mixture for analysis should be produced by the grinding and sieving processes. Samples of soil are dried in cardboard boxes at 50°C. In a mechanical mortar and pestle, the dried soil is crushed after being run through a 12-mesh (approximately 2 mm) screen. Any debris that is produced into the fine soil is removed by sieving.

2.3.4.2 Spectral Signatures of soil by using ASD FieldSpec 4

Optical instruments ASD FieldSpec 4 spectroradiometer was used to take the reflectance spectra for studying soil characteristics. The spectral response of soil is determined by several soil related characteristics such surface condition, soil texture and organic matter. Figure 2.8 Shows the soil spectral signature activities and Figure 2.9 Shows the Spectral signature Soil Graph.

(a)   **(b)**

Figure 2.8. (a) and (b) Spectral Signature of Soil using ASD FiledSpec.
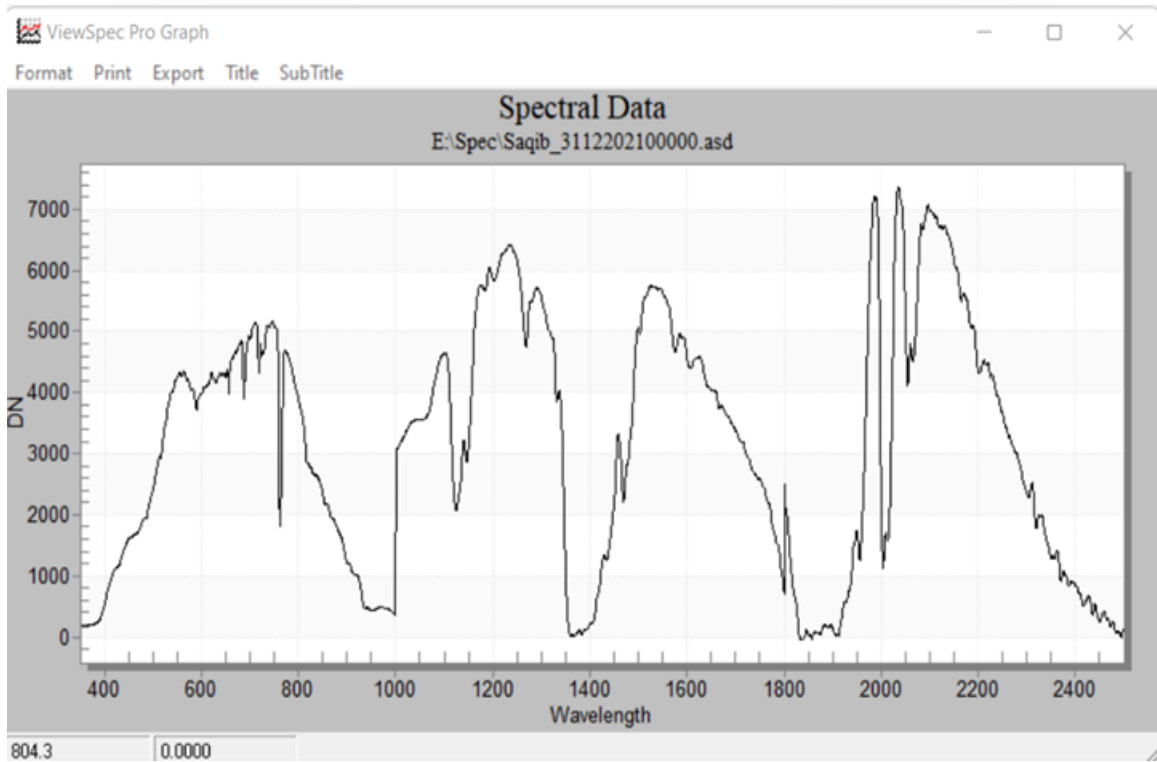
Figure 2.9. Spectral Signatures of soil.

2.3.4.3 Statistical Analysis

A multiple linear regression (MLR) analysis was performed in SAS to establish a relationship between the properties of the surface soil and satellite imagery spectral data at various wavelengths. [SAS Institute Inc., 1999]. In MLR analysis, the predictor variables are frequently chosen in earlier.it is essential to limit the set of independent variables to those that may have a physical connection to the dependent variables as including many independent variables can significantly bias the value of R^2 (Rencher and Pun, 1980).

2.3.4.4 Correlation Matrix

The Pearson Product Moment Coefficient, also known as Pearson's r, was calculated to find the potential predictors for the dependent variable. The coefficient provides a value between -1 and +1 and shows the degree of association between two variables. A strong negative or positive correlation is indicated by values that are close to extreme values. The significance of "r," however, is based on the size of the sample space and the level of significance (Lomax, 2007).

2.3.4.5 Multicollinearity

The significance of the predictor variables was then confirmed, and then check the multicollinearity statistics in data. When the predictor variables have a high degree of correlation with one another, the situation is described to as multicollinearity. When determining the contribution of each individual predictor, multicollinearity is a problem. The regression coefficient's variance may increase as a result, or the coefficient may have the incorrect signs. (Greene 2008). Any inference is therefore unreliable, and the confidence interval widens. Multi - collinearity can be found by calculating the tolerance and variance inflation factor (VIF). Eq. (2) and (3) provide the formulas for the two variables.

$$tolerance = 1 - Rj2 \quad \ldots\ldots\ldots\ldots\ldots Eq.\ (2).$$

$$VIF = (1\ /\ tolerance) \ldots\ldots\ldots\ldots\ldots\ Eq.\ (3).$$

where:

The regression coefficient for a jth predictor on all other predictor variables is Rj2. In general, a multicollinearity issue is present when the tolerance is less than 0.20 and/or the VIF is higher than 7.5. (Peat and Barto, 2005).

2.3.4.6 Multivariate Linear Regression (MLR) analysis

Multiple linear regression is used to determine the relationship between several explanatory factors and a single dependent factor, multiple linear regression is used. The variables Independent or explanatory variables are the variables we use to make predictions about the value of the dependent variable, whereas the dependent variable is the variable we are trying to predict.

Formula and Calculation of Multiple Linear Regression

$$y = b1x1 + b2x2 \ldots + bncn + c \ldots\ldots\ldots\ldots\ldots\ldots Eq.\ (4).$$

Where: y is the dependent variable, x1 is the explanatory variables, c is the slop coefficient for each explanatory variable. Multiple linear regression is a function that allows an analyst or statistician to make predictions about variable based on the information that is known about others variable. Multiple linear regression can be used when one dependent variable and several explanatory variables. The independent variables are the parameter that is used to calculate the dependent variable or outcome.

2.3.5 Implementation of USDA Textural triangle in GIS

The surface soil texture variables and soil OM were spatially modelled using the multivariate regression equations that the statistical analysis produced. The USDA textural triangle was implemented in a GIS domain to create a soil surface texture map from the sand, silt, and clay textural variables.

The procedure was completed in the following steps: The first step involved defining the upper and lower bounds for each textural class's variables. The three textural variables in the USDA textural triangle define the boundaries for each class. We essentially define the area that a specific textural class grasp within the textural triangle by applying the boundary conditions. Table 1 shows the three textural variables' limiting values for the eight textural classes that define the area of the triangle. But for some classes, the boundary lines behave differently than the normal boundary lines of the soil textural variables which is passing through the triangle, such as when the "sandy loam" class is specified. The area that the three textural variables' boundary conditions for the sandy loam class have defined is shown in Figure 2.10. it can be seen, the special area for the sandy loam class also includes some portions of many other classes. This is due to the boundary lines' deviation from the normal boundary lines of sand percent passing through the triangle. We must therefore research the boundary lines' deviating behaviors to precisely define the area of such textural classes. Similar issues arise when defining the regions classified as "loamy sand," "silt loam," and "sand." In these classes, numerical meanings were assigned to the boundary line deviating behaviors, as shown in Table 2 and boundary conditions of soil textural classes in USDA textural triangle for special cases, as shown in Table 3.
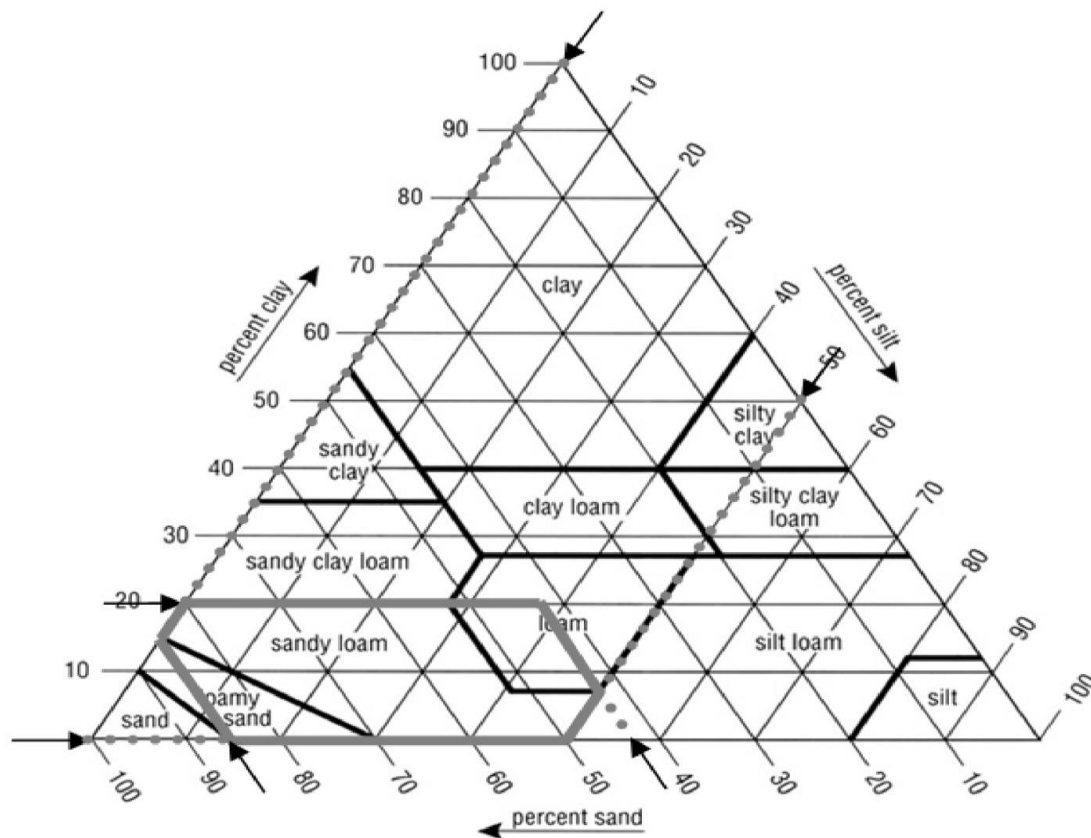
Figure 2.10. USDA soil texture triangle.

Table 2. Limiting values of textural variables for eight textural classes.

Textural Class	Sand%	Silt%	Clay%
Clay	0 to 45	0 to 40	40 to 100
Sandy Clay	5 to 65	0 to 20	35 to 55
Silt Clay	0 to 20	40 to 60	40 to 60
Sandy clay loam	45 to 80	0 to 28	20 to 35
Clay loam	20 to 45	14 to 53	27 to 40
Silt clay loam	0 to 20	40 to 74	27 to 40
Loam	23 to 53	27 to 50	7 to 27
Silt	0 to 20	80 to 100	0 to 12

Table 3. Boundary conditions of soil textural classes in USDA textural triangle for special cases.

Textural Class	Condition 1	Condition 2
Sand	a) sand (%): ≥ 85 b) [silt (%) + 1.5*clay (%)] ≤ 15	
Loamy sand	a) sand (%): $85 - 90$ b) [silt (%) + 1.5*clay (%)] ≥ 15	a) sand (%): $70 - 85$ b) [silt (%) + 2.0*clay (%)] ≤ 30
Sandy loam	a) clay (%): ≤ 20 b) sand (%): ≥ 52 c) [silt (%) + 2.0*clay (%)] ≤ 30	a) clay (%): < 7 b) silt (%): < 50 c) sand (%): $43 - 52$
Silt loam	a) silt (%): ≥ 50 b) clay (%): $12 - 27$	a) silt (%): 50-80 b) clay (%): < 12

Then, from the raster surfaces variable (i.e., sand%, silt%, clay%, (silt% + 1.5*clay%), and (silt% + 2.0*clay%)) that met the requirements for a specific soil textural class, the pixels that satisfied those criteria were extracted.

- The following step involved choosing those extracted variable pixels where each boundary condition for a specific textural class was satisfied. ArcGIS software employed the Boolean operator "AND" for this.

- The takeout variable pixels were first re-classified and given the value "1" in order to use the Boolean operator. After that, a specific textural class extracted and reclassified variable pixels were combined using the "AND" operator. This had the effect of causing all the variable pixels to have the value "1," or only those pixels to have a true value. The textural class for which the process was performed received the pixels with a value of "True" as a result. In this way, each textural class's pixel was carefully examined.

- Finally, A single soil texture map was generated by combining the pixels under each textural class. In ArcGIS software, a final surface (a depth of 7cm) soil texture map was created.

RESULTS AND DISCUSSION

3.1 Descriptive Statistics of Soil Properties

In descriptive statistics, summary statistics are used to provide an overview of the sample data and the main points of the information. Table 4 shows the descriptive statistics of the data. In table 3 the descriptive statistics show that the min, max, mean standard deviation and skewness values calculated. A lower standard deviation (SD) indicates that the soil data are aggregated over all the mean, whereas a highest SD shows that the soil data are more scattered. In contrast, a low or high SD suggest that the data points are above or below the mean respectively. A SD that is close to zero shows that the soil data points are closer to the mean. According to the conclusion the data appear to be symmetrical if the skewness ranges from -0.5 to 0. The data are moderately skewed, If the skewness is between -1 and -0.5 or between 0.5 and 1, The data are considered highly skewed if the skewness is greater than or equal to 1. In our data only Organic matter data 0.0186 close to mean and normally distributed expected other variables sand% content, silt% content and clay% content with values of 3.960, 0.9454 and 3.889 respectively. Silt variable value 1.3733 shows that is positively skewed but the organic matter, sand and clay values -1.0540, 3.464 and -3.549 respectively shows that data are negatively skewed.

3.2 Statistical Modeling of Hyperspectral Spectroradiometer Data

3.2.1 Test of Association

In table 5 shows the results of Pearson correlation coefficient calculated for soil percent sand, clay and O.M. with the spectral values ASD FieldSpec spectroradiometer.

Table 4. Summary statistics of soil.

Variable	Min	Max	Mean	Std Dev	Skewness
OM (%)	0.34	0.87	0.605	0.0186	-1.0540
Sand (%)	30	54	33.585	3.960	3.464
Silt (%)	36	42	37.618	0.9454	1.3733
Clay (%)	9	31	28.797	3.889	-3.549

Table 5. Pearson correlation coefficient between soil percent sand, clay and O.M. with the spectral values ASD FieldSpec spectroradiometer.

Variable Name	Sand		Clay		O.M.	
	Correlation Coeff.	P-value	Correlation Coeff.	P-value	Correlation Coeff.	P-value
X1362	**0.9628**	0.004	-	-	-	-
X1366	0.4770	0.0582	-	-	-	-
X1843	**0.8781**	0.0026	-	-	-	-
X1856	**0.9348**	0.0009	-	-	-	-
X1830	-	-	**0.8875**	0.0022	-	-
X1839	-	-	0.6799	0.0169	-	-
X1873	-	-	**0.8291**	0.0047	-	-
X1882	-	-	0.4940	0.0530	-	-
X1363	-	-	-	-	0.5173	0.0465
X1833	-	-	-	-	**0.9964**	0.0000
X1886	-	-	-	-	**0.9318**	0.0010
X1909	-	-	-	-	0.6989	0.0148

The percent sand variables showed a highly positive correlation with the reflection in X1362, X1366, X1843 and X 1856 at different significant levels and a strong positive correlation with the reflection in X1830, X1839, X1873 and X1882 at different significant levels. Similarly, the percent O.M. showed strong positive correlations with soil reflections in X1363, X1833, X1886 and X1909 at different significant levels.

3.2.2 Multicollinearity Test

In table 6 shows the tolerance and VIF values for multicollinearity statistics that were determined for the independent variables of sand, clay, and Organic Matter percentages. VIF of the percent sand, clay and Organic Matter predictor variables and tolerance values were well below the threshold points, so all the variables used for modeling equations.

3.2.3 Multivariate Linear Regression Equations

Multiple linear regression equations were developed using the variables that were found to be free of the multicollinearity problem. A 'stepwise 'method was used in Statistical Analysis System for selection of variables. The multivariate regression equations that resulted are given table 7.

The notably high values of R^2 examined for all soil characteristics show the importance of ASD FielsSpec spectroradiometer data in modelling variability of soil surface properties. The differences between the values of R - squared and adjusted R - squared, which is also very small, shows that the predictor variables fully account for the variability in the dependent variables. (Nanni and Dematte 2006) conducted a study to investigate the characteristics of the soil. (Thomasson et al. 2001), (Hong et al. 2002) and (Maselli et al. 2008), also taken similar statistical approach for the modelling of soil surface attributes.

Table 6. Tolerance and variance inflation factor (VIF) calculated for variables having significant correlations with the soil attributes under study.

Variable Name	Sand		Clay		O.M.	
	VIF	Tolerance	VIF	Tolerance	VIF	Tolerance
X1362	2.0463	0.488	-	-	-	-
X1366	2.0338	0.4917	-	-	-	-
X1843	1.1612	0.8612	-	-	-	-
X1856	1.1912	0.8395	-	-	-	-
X1830	-	-	1.5133	0.6608	-	-
X1839	-	-	1.0736	0.9314	-	-
X1873	-	-	1.0239	0.9767	-	-
X1882	-	-	1.4012	0.7137	-	-
X1363	-	-	-	-	1.1385	0.8784
X1833	-	-	-	-	1.2064	0.7936
X1886	-	-	-	-	15903	0.3712
X1909	-	-	-	-	1.1655	0.1420

Table 7. Resulting multivariate linear regression equations.

Variables	Equation	R	Adjusted R	RMSE
Sand (%)	Sand (%) =24.58 + (0.48 * X1362) – (0.23 * X1366) – (0.072 *X1843) + (0.08 * X1856)	0.3700	0.3140	5.8143
Silt (%)	Silt (%) =34.87– (0.018 * X1837) – (0.010 *X1912)	0.4447	0.3953	2.0231
Clay (%)	Clay (%) =39.04 – (0.077 * X1830) + (0.065 * X1839) + (0.072 *X1873) + (0.041 * X1882)	0.3165	0.2557	6.3892
O.M. (%)	OM (%) =0.98 – (0.004 * X1363) + (0.0022 *X1833) – (0.0011 * X1886) + (0.001 * X1909)	0.4402	0.3904	0.1336

3.3   Statistical Modeling of LandSat-8 OLI

3.3.1   Test of Association

The results of the Pearson correlation coefficient calculated for the percentages of sand, clay, and O.M. in the soil and the spectral values of the Landsat-8 OLI bands are shown in Table.8.

In all bands, the percent sand and clay parameters showed a significant ($p < 0.05$) positive correlation with the explanation. A similar methodology was taken by Salisbury and (D' Aria 1992), (Coleman et al. 1993) and (Barnes and Baker 2000). However, there were significant ($p < 0.05$) negative correlations between the percent O.M. and soil reflection in bands. The negative association of surface soil organic matter for each band is because as the percent of organic matter in soil increases, the soil appears darker in color, reducing overall reflectance. (Coleman and Montgomery 1987), (Galvao and Vitorello 1998), (Barnes et al. 2003), and (Ladoni et al. 2010) all reported similar findings.

3.3.2   Multicollinearity Test

In table 9 shows the tolerance and VIF values for multicollinearity statistics that were determined for the predictor variables of sand, clay, and O.M. percentages. The variance inflation factor and tolerance values for the dependent variables of percent sand, clay and O.M were estimated for band-2, band-3, band-4 and band-6 exceed the limits, implying a multicollinearity issue. The variance inflation factor and tolerance values for the dependent variables of percent sand, clay and O.M. were well within the limits for band 5,7 and 11. Consequently, these variables were removed from the analysis, and MLR analysis was performed using the remaining variables.

3.3.3 Multivariate Linear Regression Equations

Multiple linear regression equations were developed using the variables that were found to be free of the multicollinearity problem. A 'stepwise 'method was used in Statistical Analysis System for selection of variables. The multivariate regression equations that resulted are given in Table 10. The notably high values of R^2 examined for all soil characteristics show the importance of Landsat-8 OLI data in modelling variability of soil surface properties. The differences between the values of R - squared and adjusted R - squared, which is also very small, shows that the predictor variables fully account for the variability in the dependent variables. (Nanni and Dematte 2006) conducted a study to investigate the characteristics of the soil. (Thomasson et al. 2001), (Hong et al. 2002) and (Maselli et al. 2008), also taken similar statistical approach for the modelling of soil surface attributes. The use of LandSat-8 OLI data, they also done multiple linear regression analysis and investigated R^2 values of 0.589 and 0.687 for clay % content and soil organic matter % content respectively. (Thomasson et al. 2001), (Hong et al. 2002) and (Maselli et al. 2008), also created similar statistical methods for simulating soil attributes.

Table 8. Pearson correlation coefficient (r) between Landsat-8 OLI bands spectral values and percent sand, clay, and O.M.

Variable Name	Clay	Sand	O.M.
Band2	0.696	0.627	-0.513
Band3	0.724	0.492	-0.447
Band4	0.742	0.495	-0.359
Band51	0.509	0.245	-0.308
Band6	0.732	0.567	-0.319
Band7	0.648	0.523	-0.366
Band11	-0.275	0.118	-0.023

At significance level (p< 0.05)

Table 9. Tolerance and Variance Inflation Factor (VIF) calculated for variables having significant correlations with the soil attributes under study.

Variable Name	Sand		Clay		O.M.	
	VIF	Tolerance	VIF	Tolerance	VIF	Tolerance
Band2	**18.498**	0.054	**18.498**	0.054	**18.498**	0.054
Band3	**56.846**	0.018	**56.846**	0.018	**56.846**	0.018
Band4	**36.521**	0.027	**36.521**	0.027	**36.521**	0.027
Band5	5.023	0.199	5.023	0.199	5.023	0.199
Band6	**12.192**	0.082	**12.192**	0.082	**12.192**	0.082
Band7	6.707	0.149	6.707	0.149	6.707	0.149
Band11	1.868	0.535	1.868	0.535	1.868	0.535

(Values in bold exceed the threshold values > 7.5).

Table 10. Resulting multivariate linear regression equations.

Variables	Equation	R^2	Adjusted R^2	RMSE
Sand (%)	Sand(%)= 28.86(1.50*band_5)-(3.18*band_7) +(1.05*band_11)	0.558	0.553	0.432
Clay (%)	Clay(%) = 28.05-(3.18*band_5)-(2.61*band_7) +(1.38*band_11)	0.589	0.584	0.287
O.M. (%)	OM_N = 0.48-(5.66*band_5) -(2.23*band_7) +(1.68*band_11)	0.687	0.683	0.010

3.4   Spatial Modeling

As a result, clay, sand, and O.M. multivariate regression equations are used to spatial model these spatial variables. Figure 3.1 Shows the spatial variable bare soil band 5, Figure 3.2 shows the spatial variable bare soil band 7 and Figure 3.3 shows the spatial variable bale soil band11. The results indicated that the percent sand observed ranged from 30 to 54 % in the study area. here we check that maximum value fall in range of 30.12 to 33.31 in the north and mid of the study area and values 39.69 to 53.34 in south side of the study area this is due to river side, in clay map values varied from 9 to 31 and maximum values spread in between 28.47 to 30.98 all over the study area, in silt map values varied from 36.01 to 41.76 and maximum value varied from 36.01 to 37.96 in this study area . Figure 3.4 shows the sand percent map. Figure 3.5 shows the clay percent map and Figure 3.6 shows silt percent map.

3.5   Generate Soil Texture Map by Using USDA Textural Triangle

study area's soil texture map was created by combining the soil texture factors. The "clay loam" class was the most prevalent textural class inside the study area, followed by the "loam" class, according to the values of number of pixels count for the measured textural classes. Figure 3.7 despite the Spatial soil surface texture distribution.

The soil texture-values distribution graph shows the soil of Shakargarh. The "clay loam" class was the most prevalent textural class inside the study area, followed by the "loam" class, according to the values of number of pixels count for the observed textural classes. The soil of the study area is densely compacted together with each other with very little or no airspace. This soil seems to have excellent water storage characteristics and makes it hard for air and moisture to penetrate it. It is very moist to the touch when moisture but soft when dried.
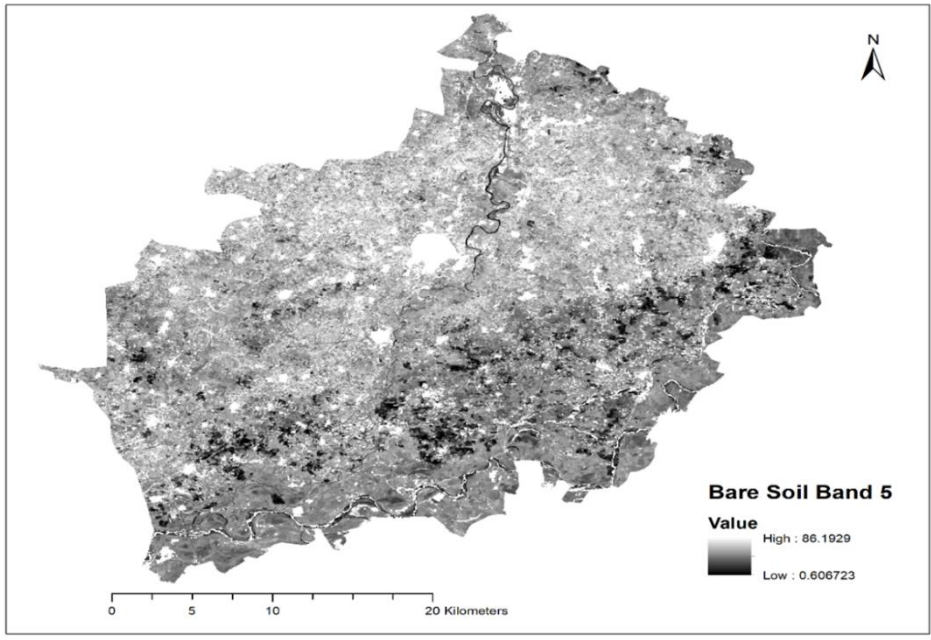
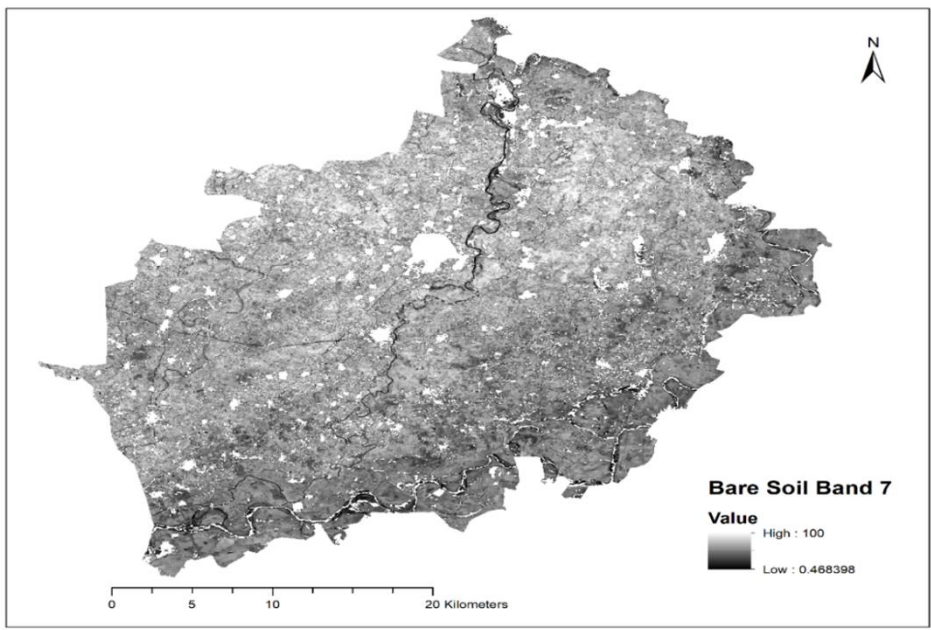Figure 3.1. Spatial variable bare soil band 5.

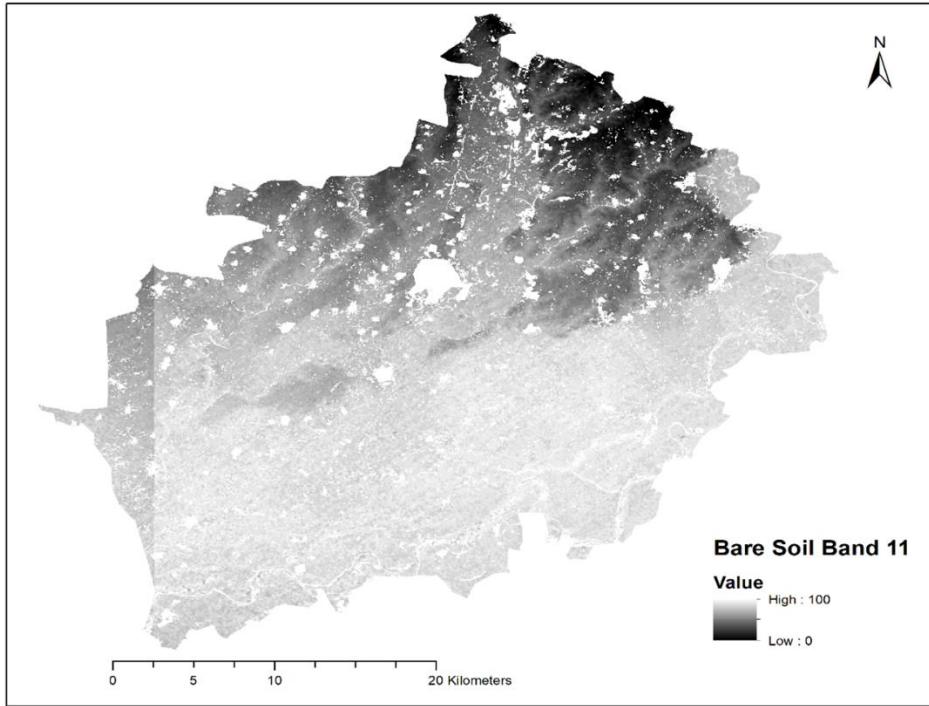Figure 3.2. Spatial variable bare soil band 7.

Figure 3.3. Spatial variable bare soil band 11.
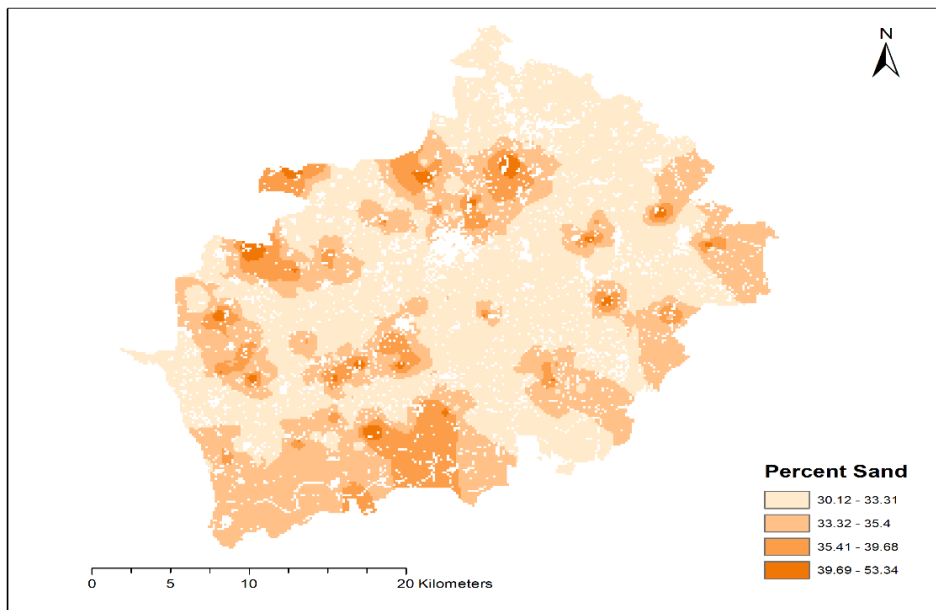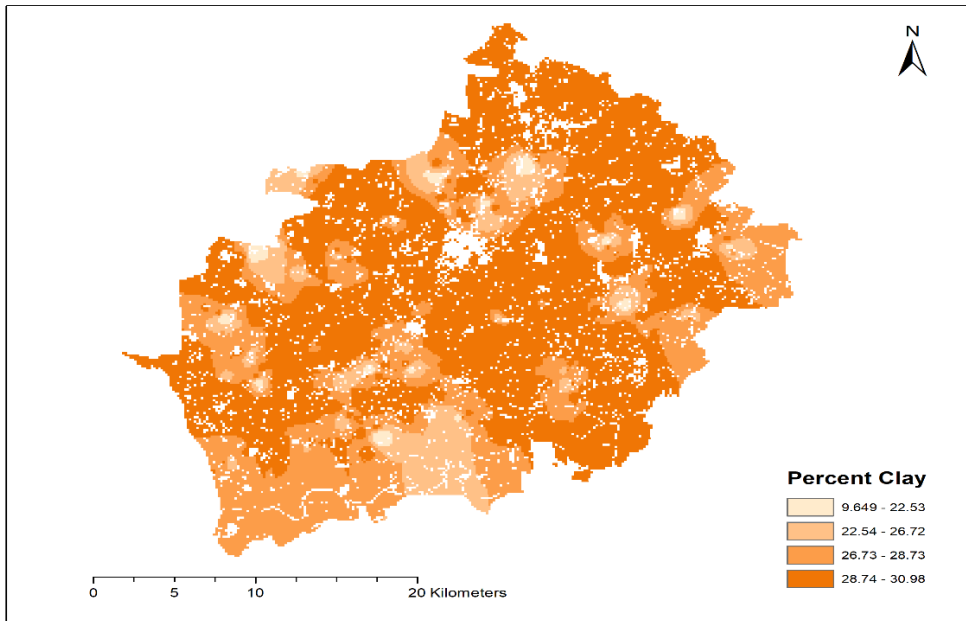

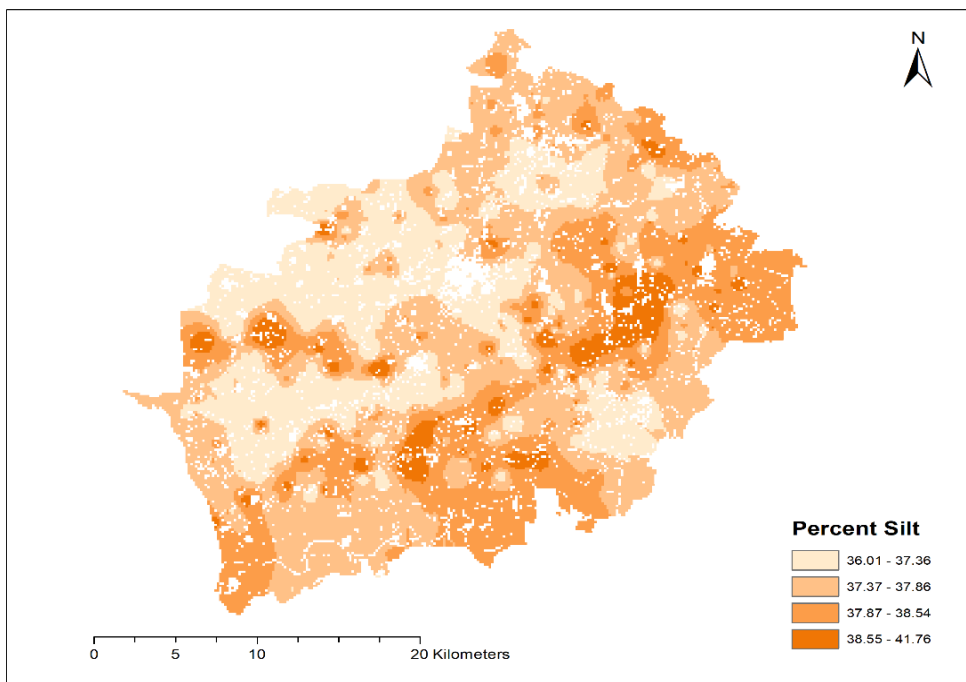Figure 3.4. Sand percent map.

Figure 3.5. Clay percent map.

Figure 3.6. Silt percent map.

3.6 Generate Soil Organic Matter Map

Organic matter map of the study area prepared by using spatial model. Values varied in the organic matter map from 0.34 to 0.87. Most extensive values in the North were found to range from 0.3 to 0.41 percent, organic matter in this area is very low condition, and in the South side values spread in this area from 0.42 to 0.87 percent. Organic matter in this area is some batter condition. The spatial variability of soil organic matter is shown in Figure 3.8.

3.7 Data Validation

To assess the accuracies of spatial modelling, 25 evenly distributed soil surface samples (not part of the analysis) were selected for validation. It was attempted to compare the measured values of the soil profile characteristics to the calculated results. RMS error was calculated for each of the soil parameter models. The measured RMS errors for percent sand, clay, and O.M. were found to be 0.432, 0.287, and 0.010, respectively.
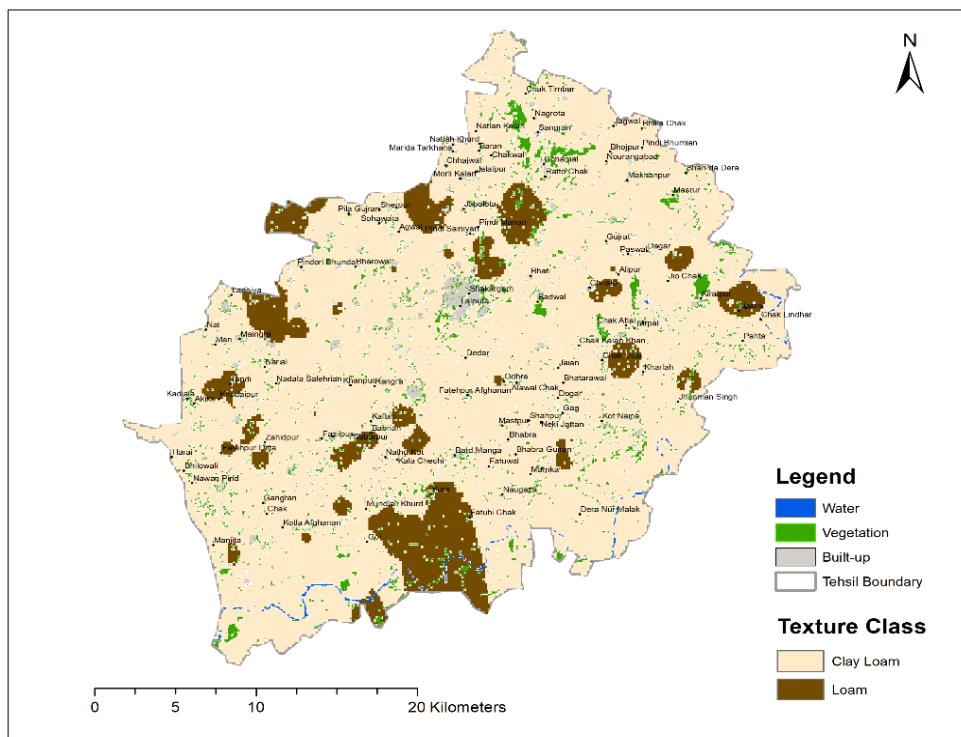
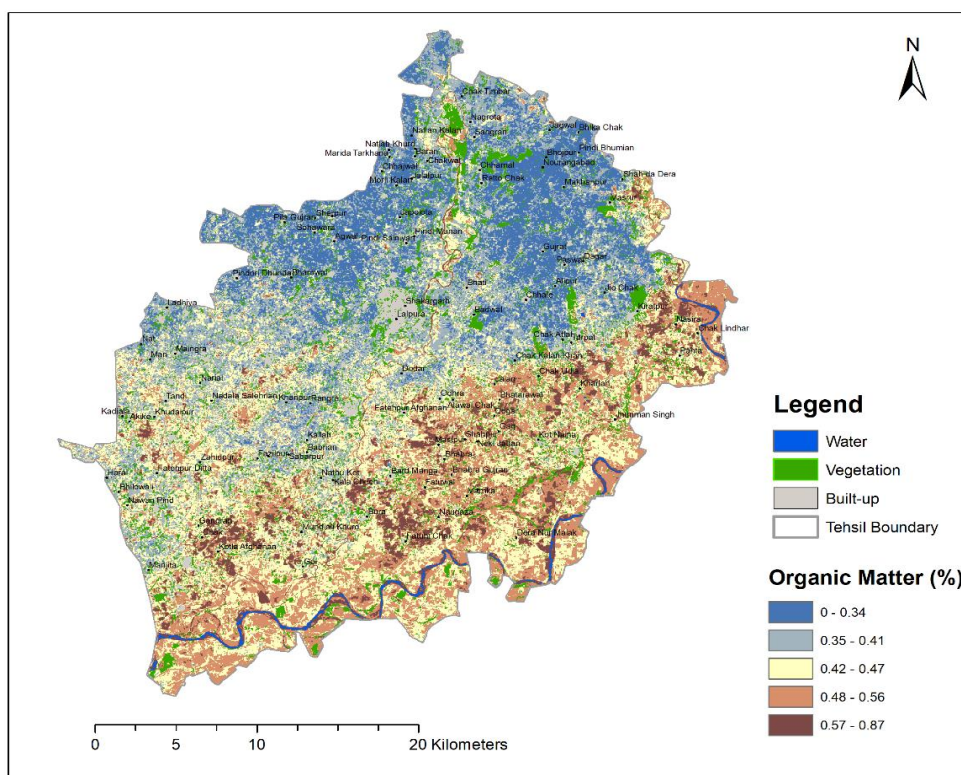Figure 3.7. Spatial distribution of surface soil texture.

Figure 3.8. Spatial distribution of surface soil O.M

CONCLUSION AND RECOMMENDATIONS

Fine level spatial variation analysis and modelling of large area soil surface characteristics are possible using remote sensing satellite data (imagery and non-imagery), as most of these soil surface characteristics, such as soil texture and O.M., influence soil reflectance directly or indirectly. The spectral reflectance values data can be used instead of the conventional techniques to identify soil attributes. A MLR techniques has been except for studying the relationship between soil surface properties and hyperspectral non-imagery data which revealed wavelength X1362, X1366, X1843 and X1856 as the best predictors of percent sand, wavelength X1830, X1839, X1873 and X1882 as the most accurate predictors of clay content, wavelength X1837 and 1912 as the best predictors of percent silt and wavelength X1363, X 1833, X1886 and X1909 as the best predictors of percent O.M. The best predictors of the percentage of sand, clay, and O.M. were bands 5, 7 and 11, according to the relationship between soil surface properties and soil reflectance. The USDA soil textural triangle has been used to perform spatial modelling of soil texture. The findings identified "clay loam" and "loam" as the two primary soil texture classes in the study area. Additionally, very little (>1%) O.M. status was found in the study area.

4.1 RECOMMENDATIONS

i.   Traditional practices for soil mapping are outdated and must be replaced by Remote Sensing approaches.

ii. Modelling approaches for soil prediction must be replaced by Geospatial Statistics, GIS Models and Artificial Neural Network.

iii. Satellite Images with high spectral and spatial resolution can further improve this research subjected to cost.

REFERENCES

1.   Ahmed, Z., & Iqbal, J. (2014). Evaluation of Landsat TM5 multispectral data for automated mapping of surface soil texture and organic matter in GIS. *European Journal of Remote Sensing*, *47*(1), 557–573. https://doi.org/10.5721/EuJRS20144731

2.   Alexakis, D. D., Tapoglou, E., Vozinaki, A. K., & Tsanis, I. K. (2019). *Integrated Use of Satellite Remote Sensing , Artificial Neural Networks , Field Spectroscopy , and GIS in Estimating Crucial Soil Parameters in Terms of Soil Erosion*.

3.   Ali, M., Iqbal, I. M., Shabbir, A., Khan, Z. U. D., & Khan, M. T. A. (2020). Ethnomedicinal studies on aquatic plants of tehsil Shakargarh, Punjab, Pakistan. Journal of Medicinal Plants, 8(1), 15-19.

4.   Baodong M., Lixin W., Shanjun L. (2008) - Remote Sensing Detection of Subsidence-Resulted Water Body and Solid-Waste Dump In Coal Mine: Yanzhou Being a Case. The International Archives of the Photogrammetry, Remote Sensing and Spatial Information Sciences, 37: 269-272.

5.   Barnes E.M., Baker M.G. (2000) - Multispectral Data For Mapping Soil Texture:Possibilities and Limitations. Applied Engineering in Agriculture, 16 (6): 731-741. doi:http://dx.doi.org/10.13031/2013.5370

6.   Baumgardner M.F., Silva L.F., Biehl L.L., Stoner E.R. (1986) - Reflectance Propertiesof Soils.Advances in Agronomy, 38: 1-44. doi: http://dx.doi.org/10.1016/S0065-2113(08)60672-0

7.   Beuselinck, L., Govers, G., Poesen, J., Degraer, G., & Froyen, L. (1998). Grain-size analysis by laser diffractometry: comparison with the sieve-pipette method. Catena, 32(3-4), 193-208.

8.   Bousbih, S., Zribi, M., Pelletier, C., Gorrab, A., Lili-Chabaane, Z., Baghdadi, N., Aissa, N. Ben, & Mougenot, B. (2019). Soil texture estimation using radar and optical data from Sentinel-1 and Sentinel-2. *Remote Sensing*, *11*(13). https://doi.org/10.3390/rs11131520

9.   Ben-Dor E., Banin A. (1995) - Near-infrared analysis as a rapid method to simultaneouslyevaluate several soil properties. Soil Science Society of America Journal, 59: 364-372.doi: http://dx.doi.org/10.2136/sssaj1995.03615995005900020014x

10.   Brown R.B. (2003) - Soil Texture [Fact Sheet]. Retrieved from http://edis.ifas.ufl.edu/ss169

11.   Czapla-Myers, J., McCorkel, J., Anderson, N., Thome, K., Biggar, S., Helder, D., Aaron, D., Leigh, L., & Mishra, N. (2015). The ground-based absolute radiometric calibration of Landsat 8 OLI. *Remote Sensing*, *7*(1), 600–626. https://doi.org/10.3390/rs70100600.

12.   Coleman T.L., Agbu P.A., Montgomery O.L. (1993) - Spectral differentiation on surfacesoils and soil properties: Is it possible from space platforms? Soil Science, 155: 283-293. doi: http://dx.doi.org/10.1097/00010694-199304000-00007.

13. Coleman T., Montgomery O. (1987) - Soil moisture, organic matter and iron content effect onspectral characteristics of selected Vertisols and Alfisols in Alabama. PhotogrammetricEngineering and Remote Sensing, 53: 1659-1663.

14. Daniel K.W., Tripathi N.K., Honda K., Apisit E. (2004) - Analysis of VNIR (400-1100 nm)

15. Day P.R. (1965) - Particle Fractionation and Particle-Size Analysis. In: Method of SoilAnalysis, Black C.A. (Ed), PartI, Soil Science Society of America Journal.

16. Dwivedi R.S. (2001) - Soil Resource Mapping: A Remote Sensing Perspective. RemoteSensing Reviews, 20: 89-122. doi: http://dx.doi.org/10.1080/02757250109532430.

17. Estimating Within-Field Variations In Soil Properties From Airborne Hyperspectral Images. In: Pecora 15/Land Satellite Information IV Conference, 10-15 November, (Colorado: ASPRS), pp. 10-15

18. Ehsani M.R., Upadhyaya S.K., Slaughter D., Shafii S., Pelletier M. (1999) - A NIR Techniquefor Rapid Determination of Soil Mineral Nitrogen. Precision Agriculture, 1 (2): 217-234. doi: http://dx.doi.org/10.1023/A:1009916108990.

19. Ge, Y., Thomasson, J. A., & Sui, R. (2011). Remote sensing of soil properties in precision agriculture: A review. *Frontiers of Earth Science*, *5*(3), 229–238. https://doi.org/10.1007/s11707-011-0175-0

20. Gholizadeh, A., Žižala, D., Saberioon, M., & Borůvka, L. (2018). Soil organic carbon and texture retrieving and mapping using proximal, airborne and Sentinel-2 spectral imaging. *Remote Sensing of Environment*, *218*(September), 89–103. https://doi.org/10.1016/j.rse.2018.09.015

21. Galvao L.S., Vitorello I. (1998) - Role of organic matter in obliterating the effects of iron onspectral reflectance and color of Brazilian tropical soils. International Journal of RemoteSensing, 19 (10): 1969-1979. doi: http://dx.doi.org/10.1080/014311698215090.

22. Galvao L.S., Vitorello Í., Roberto A. (1997) - Relationships of spectral reflectance andcolor among surface and subsurface horizons of tropical soil profiles. Remote Sensingof Environment, 61 (1): 24-33. doi: http://dx.doi.org/10.1016/S0034-4257(96)00219-2.

23. Gilabert M.A., Conese C., Maselli F. (1994) - An atmospheric correction method for theautomatic retrieval of surface reflectances from TM images. International Journal of Remote Sensing, 15: 2065-2086. doi: http://dx.doi.org/10.1080/01431169408954228.

24. Greene W.H. (2008) - Econometric Analysis. Fourth edition, New Delhi: Dorling Kindersley,India, pp. 56-61.

25. Hashemi S.S., Baghernejad M., Pakparvar M. (2007) - GIS Classification Assessment for Mapping Soils by Satellite Images. In: 4th Middle East Spatial Technologies

Conferenceand Exhibition, 10-12 December 2007, Bahrein.

26. Haider, S., Ashraf, E., & Javed, M. A. (2016). Assessment of Factors Causing Lack of Interest among Small-Scale Farmers in Agriculture System in Tehsil Shakargarh, Pakistan. PSM Biological Research, 1(2), 53-57.

27. Hocking R.R. (1976) - The analysis and selction of variables in linear regression. Biometrics, 32: 1-49. doi: http://dx.doi.org/10.2307/2529336.

28. Hoffer R. (1978) - Biological and physical considerations in application computer aided analysis techniques to remote sensing. In: Remote Sensing: The Quantitative Approach,Swain P.H., & Davis S.M. (Eds.), pp. 237-286 (New York: McGraw-Hill).

29. Hong S.Y., Sudduth K.A., Kitchen N.R., Drummond S.T., Palm H.L., Wiebold W.J. (2002)

30. Jensen J.R. (2000) - Remote Sensing of The Environment. Singapore: Pearson Education, pp. 507-515.

31. Hummel J.W., Sudduth K.A., Hollinger S.E. (2001) - Soil moisture and organic matter prediction of surface and subsurface soils using an NIR soil sensor. Computers and Electronics in Agriculture, 32 (2): 149-165. doi: http://dx.doi.org/10.1016/S0168-1699(01)00163-6.

32. Jensen J.R. (2000) - Remote Sensing of The Environment. Singapore: Pearson Education,pp.507-515.

33. Karaburun A. (2010) - Estimation of C factor for soil erosion modeling using NDVI in Buyukcekmece watershed. Ozean Journal of Applied Sciences, 3 (1): 77-85.

34. Krishnan P., Butler B.J., Hummel J.W. (1981) - Close-range sensing of soil organic matter.Transactions of the American Society of Agricultural Engineers (ASAE), 24 (2): 306-311. doi: http://dx.doi.org/10.13031/2013.34246.

35. Levy, J., Nolin, A., Fountain, A., & Head, J. (2014). Hyperspectral measurements of wet, dry and saline soils from the McMurdo Dry Valleys: Soil moisture properties from remote sensing. *Antarctic Science*, *26*(5), 565–572. https://doi.org/10.1017/S0954102013000977

36. Liao, K., Xu, S., Wu, J., & Zhu, Q. (2013). Spatial estimation of surface soil texture using remote sensing data. *Soil Science and Plant Nutrition*, *59*(4), 488–500. https://doi.org/10.1080/00380768.2013.802643

37. Lomax R.G. (2007) - An introduction to statistical concepts. New Jersey: Lawrence Erlbaum Associates, pp. 182-188.

38. Ladoni M., Bahrami H.A., Alavipanah S.K., Norouzi A.A. (2010) - Estimating soil organiccarbon from soil reflectance:a review. Precision Agriculture, 11 (1): 82-99. doi: http://dx.doi.org/10.1007/s11119-009-9123-3.

39. Luo Z., Yaolin L., Jian W., Jing, W. (2008) - Quantitative mapping of soil organic materialusing field spectrometer and hyperspectral remote sensing. The International Archives

ofthe Photogrammetry, Remote Sensing and Spatial Information Sciences, 37: 901-906.

40.   Mirzaee, S., Ghorbani-Dashtaki, S., Mohammadi, J., Asadi, H., & Asadzadeh, F. (2016). Spatial variability of soil organic matter using remote sensing data. *Catena*, *145*, 118–127. https://doi.org/10.1016/j.catena.2016.05.023

41.   Manchanda M.L., Kudrat M., Tiwari A.K. (2002) - Soil survey and mapping using remotesensing. Tropical Ecology, 43 (1): 61-74.

42.   Maselli F., Gardin L., Bottai L. (2008) - Automatic mapping of soil texture through theintegration of ground, satellite and ancillary data. International Journal of RemoteSensing, 29 (19): 5555-5569. doi: http://dx.doi.org/10.1080/01431160802029651.

43.   Mulla D.J., Sekely A.C., Beatty M. (2000) - Evaluation of remote sensing and targeted soil sampling for variable rate application of lime. In: Proceedings of the 5th International Conference on Precision Agriculture, 16-19 July 2000, Bloomington, pp. 1-14.

44.   Nanni, M. R., & Demattê, J. A. M. (2006). Spectral Reflectance Methodology in Comparison to Traditional Soil Analysis. *Soil Science Society of America Journal*, *70*(2), 393–407. https://doi.org/10.2136/sssaj2003.0285

45.   Okin G.S., Painter T.H. (2004) - Effect of grain size on remotely sensed spectral reflectance of sandy desert surfaces. Remote Sensing of Environment, 89: 272-280. doi: http://dx.doi.org/10.1016/j.rse.2003.10.008.

46.   Palacios-Orueta A., Ustin S.L. (1998) - Remote Sensing of Soil Properties in the Santa Monica Mountains I. Spectral Analysis. Remote Sensing of Environment, 65 (2): 170-183. doi: http://dx.doi.org/10.1016/S0034-4257(98)00024-8.

47.   Peat J.K., Barto B. (2005) - Medical statistics: a guide to data analysis and critical appraisa. Oxford: Blackwell Publishing Ltd., pp. 172-173. doi: http://dx.doi.org/10.1002/97804 70755945

48.   Rembold, F., Meroni, M., Urbano, F., Royer, A., Atzberger, C., Lemoine, G., ... & Haesen, D. (2015). Remote sensing time series analysis for crop monitoring with the SPIRITS software: new functionalities and use examples. Frontiers in Environmental Science, 3, 46.

49.   Rencher A.C., Pun F.C. (1980) - Inflation of R2 in Best Subset Regression. Technometrics, 22: 49-54. doi: http://dx.doi.org/10.2307/1268382.

50.   Ren, C., Liu, S., Van Grinsven, H., Reis, S., Jin, S., Liu, H., & Gu, B. (2019). The impact of farm size on agricultural sustainability. Journal of Cleaner Production, 220, 357-367.

51.   SAS Institute Incorporation (1999) - SAS/STAT User's Guide, Version 8, Cary, NC : SAS Institute Incorporation

52.   Schumacher, B. A. (2002). Methods for the determination of total organic carbon (TOC)in soils and sediments.

53.	Shahriari, M., Delbari, M., Afrasiab, P., & Pahlavan-Rad, M. R. (2019). Predicting regional spatial distribution of soil texture in floodplains using remote sensing data: A case of southeastern Iran. *Catena*, *182*(June), 104149. https://doi.org/10.1016/j.catena.2019.104149

54.	Shepherd K., Walsh M. (2002) - Development of reflectance spectral libraries for characterization of soil properties. Soil Science Society of America Journal, 66: 988-998. doi: http://dx.doi.org/10.2136/sssaj2002.0988.

55.	Spectral signatures for estimation of soil organic matter in tropical soils of Thailand.International Journal of Remote Sensing, 25: 643-652. doi: http://dx.doi.org/10.1080/0143116031000139944

56.	Song, Y. Q., Yang, L. A., Li, B., Hu, Y. M., Wang, A. Le, Zhou, W., Cui, X. Sen, & Liu, Y. L. (2017). Spatial prediction of soil organic matter using a hybrid geostatistical model of an extreme learning machine and ordinary kriging. *Sustainability (Switzerland)*, *9*(5). https://doi.org/10.3390/su9050754

57.	Tariq, S. R., & Rashid, N. (2013). Multivariate analysis of metal levels in paddy soil, rice plants, and rice grains: a case study from Shakargarh, Pakistan. *Journal of Chemistry*, *2013*.

58.	Thomasson J.A., Sui R., Cox M.S., Al–Rajehy A. (2001) - *Soil Reflectance Sensing For Determining Soil Properties In Precision Agriculture*. Transactions of the American Society of Agricultural Engineers, 44: 1445-1453. doi: http://dx.doi.org/10.13031/2013.7002.

59.	Vibhute, A. D., Dhumal, R. K., Nagne, A., Surase, R., Varpe, A., Gaikwad, S., Kale, K. V., & Mehrotra, S. C. (2018). Assessment of soil organic matter through hyperspectral remote sensing data (VNIR spectroscopy) using PLSR method. *Proceedings - 2017 2nd International Conference on Man and Machine Interfacing, MAMI 2017*, *2018-March*, 1–6. https://doi.org/10.1109/MAMI.2017.8307888

60.	ibhute, A. D., Kale, K. V., Mehrotra, S. C., Dhumal, R. K., & Nagne, A. D. (2018). Determination of soil physicochemical attributes in farming sites through visible, near-infrared diffuse reflectance spectroscopy and PLSR modeling. *Ecological Processes*, *7*(1). https://doi.org/10.1186/s13717-018-0138-4

61.	Viscarra-Rossel R.A., Mcbratney A.B. (1998) - Laboratory evaluation of a proximal sensing technique for simultaneous measurement of soil clay and water content Geoderma, A Global Journal of Soil Science, 85 (1): 19-39.

62.	Virgawati, S., Mawardi, M., Sutiarso, L., Shibusawa, S., Segah, H., & Kodaira, M. (2018). Mapping the Variability of Soil Texture-Based on Vis-NIR Proximal Sensing. *Journal of Applied Geospatial Information*, *2*(1), 108–116. https://doi.org/10.30871/jagi.v2i1.798

63.	Yu, H., Kong, B., Wang, G., Du, R., & Qie, G. (2018). Prediction of soil properties using a hyperspectral remote sensing method. *Archives of Agronomy and Soil Science*, *64*(4), 546–559. https://doi.org/10.1080/03650340.2017.1359416

64.   Walkley, A.J. and Black, I.A. (1934) Estimation of soil organic carbon by the chromic acid titration method. Soil Sci. 37, 29-38.

65.   Wen, B., Aydin, A., & Duzgoren-Aydin, N. S. (2002). A comparative study of particle size analyses by sieve-hydrometer and laser diffraction methods. Geotechnical Testing Journal, 25(4), 434-442.

66.   Zhang, Z. F. (2011). Soil water retention and relative permeability for conditions from oven dry to full saturation. *Vadose Zone Journal*, *10*(4), 1299-1308.